DOI: 10.1002/ejic.200901071

Systematic Structural Coordination Chemistry of *p-tert*-Butyltetrathiacalix[4]arene: Further Complexes of Transition-Metal Ions[‡]

Alexander Bilyk,[a] John W. Dunlop,[a] Rebecca O. Fuller,[a,b] Annegret K. Hall,[a] Jack M. Harrowfield,*[a,c] M. Wais Hosseini,[d] George A. Koutsantonis,[a] Ian W. Murray,[a] Brian W. Skelton,[a] Robert L. Stamps,[b] and Allan H. White[a]

Keywords: Calixarenes / Transition metals / Solvent inclusion / Solid-state structures

In extension of earlier work on complexes of *p-tert*-butyltetrathiacalix[4]arene, LH_4, with late transition-metal M^{II} species, we report studies of complexes modelled on the basis of single-crystal X-ray studies as derivatives of V^{V}, W^{VI}, Mn^{II}, Fe^{III}, Ni^{II}, Cu^{II} and Pd^{II}, the last as a trio of heteronuclear species also involving Ca^{II}. In complexes $[VO(OH)(LH_2)\cdot 2.5dmf\cdot 2H_2O]$ (×2) (**1**), $Cl_2W(L)\cdot 3.5C_6H_6$ (**2**) and $[Mn(LH_2)\cdot 3.5CH_2Cl_2]$ (×2) (**3**) included dmf is found only in the partially deprotonated calixarene cavities of **1** and **3**. In oligonuclear $OFe_3(HCO_2)(LH)_2\cdot 2H_2O\cdot 6dmf$ (**4**) and $2Cuac_2\cdot Cu_2(L)\cdot dmf\cdot 4.5CH_2Cl_2$ (**6**) (ac = acetate) included dmf is found in both. Ni^{II} provides several species, including **5a**, binuclear $(Et_3NH)Ni_2(LH)(LH_2)\cdot 2dmf\cdot 2Me_2CO\cdot H_2O$, **5b**, a remarkable hexanuclear (binuclear + tetranuclear) aggregate, $Ni_6(L)(LH)_2(LH_2)\cdot 4MeCN\cdot 6H_2O$, and **5c**, an even more remarkable Ni_{32} aggregate modelled as (centrosymmetric) $Ni_{32}(OH)_{40}(L)_6\cdot 8dmso\cdot 10dmf$, in which there are two sets of nickel atoms, one disposed at the corners of a cube (Ni_8), the other (Ni_{24}) at the vertices of a cuboctahedron (the Ni_8 vertices at the centres of the hexagonal faces); the hydroxy groups comprise two sets: one, $(OH)_{24}$, disposed outside the spheroidal shell of nickel atoms, the other, $(OH)_{16}$, disordered within, the thiacalixarene ligands L_6 being disposed about the axes of the octahedron. Heteronuclear species have been found as Ca^{II}/Pd^{II} combinations $CaPd_2(LH)_2\cdot 1.5CH_2Cl_2$ (**7a**), $CaPd(LH_2)\cdot 3dmso\cdot H_2O\cdot 4.5MeCN$ (**7b**), $Ca_2Pd(LH)_2\cdot 3.5dmso\cdot 1.5H_2O\cdot 4MeCN$ (**7c**), all with included solvent.

Introduction

The tendency of *p-tert*-butyltetrathiacalix[4]arene to form oligonuclear derivatives[1–3] with transition-metal ions has been established by structural studies almost entirely based on M^{II} species derived from middle to late members of the series.[3b,4–15] A common motif in these structures is a "sandwich" form in which di-, tri- or tetrametallic units are held between the quasi-planar phenolic-O_4 faces of a pair of *cone*-form calixarene entities with their ligand cavities occupied by various solvents. To extend the characterisation of this field of coordination chemistry, we have endeavoured (as have others[2,12–14]) to study a selection of derivatives involving both early members and those in oxidation states other than (II), though for us this has met with only partial success in terms of obtaining crystalline materials suitable for diffraction studies. While there is evidence, elaborated on in the associated present reports[16,17] of more general thiacalixarene coordination chemistry, that the nature of the complex which crystallises from a given synthetic mixture may be subject to somewhat capricious influences, other recent work[5b,12,13] has shown that solvothermal syntheses appear to have good reproducibility and that this method may enable access to a more complete definition of at least the solid state coordination chemistry of transition-metal ion complexes of the thiacalixarene. There is, of course, a developing chemistry of complexes of higher thiacalix[*n*]arenes as well as of thiacalix[4]arene derivatives.[2,8,10,18–28] Here, we describe structural studies of *p-tert*-butyltetrathiacalix[4]arene complexes of V^{V}, W^{VI}, Mn^{II}, Ni^{II}, Pd^{II} (as mixed-metal species involving Ca^{II}) and Cu^{II}, the last an unusual[5b] "open sandwich" complex. For the purpose of comparison, some features of previously published structures of Cu^{II}[5a] and Hg^{II}[8] species are also considered in greater detail.

Results and Discussion

As for the main group elements discussed in the preceding paper,[16] only a partial characterisation of the structures of transition-metal derivatives of *p-tert*-butyltetra-

[‡] Part III; part I: ref.[35]; part II: ref.[16]; part IV: ref.[17]

[a] Chemistry M313, School of Biomedical, Biomolecular and Chemical Sciences, University of Western Australia, Crawley, Western Australia 6009
[b] School of Physics M013, The University of Western Australia, Crawley, Western Australia 6009
[c] Laboratoire de Chimie Supramoléculaire, Institut de Science et d'Ingénierie Supramoléculaires, Université de Strasbourg, 67083 Strasbourg, France
[d] Laboratoire de Chimie de Coordination Organique, Institut Le Bel, Université de Strasbourg, 67000 Strasbourg, France

Supporting information for this article is available on the WWW under http://dx.doi.org/10.1002/ejic.200901071.

thiacalixarene has proved possible presently. The positive aspects of this work, viz. the structures actually solved, are discussed below, while some broader issues of this chemistry are left for consideration in our subsequent assessment of the overall results concerning thiacalixarene coordination.[17] A number of general observations and *caveats* presented at the beginning of the Results and Discussion section of the previous paper[16] are also pertinent to the present situation and are not reiterated. As is commonly the case with calixarene structures, in some cases the protonic hydrogen locations (Table S1) are less certain than desired and some solvent components ill-defined. Indicators of ligand conformations, coordination modes, geometries, and protonation are compared globally in Tables S1 and S2 (Supporting Information), with metal-atom environments presented in subsequent Tables (Supporting Information) and the Figures.

VO(OH)(LH$_2$)·2.5dmf·2H$_2$O (×2) ≡ [{(dmf·LH$_2$)OV(μ-*O*H)}$_2$](·3dmf·4H$_2$O) (1)

The earliest member of the first transition-metal series to provide a thiacalixarene complex as crystals suitable for a structure determination in the present study is vanadium. On the basis of its room-temperature diamagnetism (and the structure determination itself), it is formulated as a binuclear V^V species, **1**, a pair of vanadium atoms being linked by a pair of oxygen bridges, the VO_2V array being disposed about a crystallographic inversion centre (and thus planar), so that one half of the ascribedly neutral molecule (with associated, included, and lattice solvent molecules) comprises the asymmetric unit of the structure. Hydroxylic proton locations are ill-defined {two notionally located on the non-coordinating oxygen atoms of the ligand [O(31,41), directed toward O(21,11), respectively (Table S1)], none on the putative water molecules}, but the general features of the array are consistent with those given. As well, while this work was in progress, detailed studies[14] of the structures and solution chemistry of more clearly defined V^V complexes, one related to the present as a result of simple deprotonation, were published.

The vanadium atom is six-coordinate and quasi-octahedral (Figure 1, Table S3). The V–O distances range widely, with that to the terminal O(1) being the shortest by a significant margin, the bridging O(2,2′) the next and the ligand O(11,21) the longest, although the dimer in the solid is more symmetrical than its conjugate base, characterised as its tetraphenylphosphonium salt.[14] The distance to the sulfur atom, between O(11,21) and *trans* to V–O(1), is very long [2.7602(8) Å]. Charge balance, assuming the pair of phenolic hydrogen atoms H(31,41), persuasively located as directed toward O(21,11) (Table S1), to be correct, requires that the bridging O(2) is hydroxide on V^V [hydrogen atoms not located but O(2) has various other oxygen atoms at distances < 2.8 Å]. A dmf molecule is included in each calixarene cavity, penetrating by means of one of the *N*-methyl groups.

The structure of the complex unit (Figure 1) is that of a highly "slipped" sandwich, closely similar in form to the Ga^{III} complex,[16] though the crystals are not isomorphous. As in the gallium complex, the single independent calixarene ligand conformation is very close to that of a regular *cone* (Table S1, Supporting Information). Some dimensions characterising the V coordination sphere are shorter and less symmetrical than those of Ga [V–OH$_2$(bridge) 1.846(2), 1.806(2) Å cf. Ga–OH(bridge) 1.948(4) Å; V···V 2.7486(10) Å cf. Ga···Ga 3.023(2) Å; V–O 1.607(2) Å cf. Ga–O(dmf) 1.959(8) Å], whilst others are longer [V–O(calix) 1.978(2), 1.983(2) Å cf. Ga–O(calix) 1.941(5) Å], particularly V–S [2.7602(8) Å cf. Ga–S 2.548(3) Å], this last value offering some justification for regarding the calixarene on V^V as a bidentate O_2 donor rather than a tridentate O_2S *fac*-tripod species, and the vanadium atom therefore as five- and not six-coordinate. This bond elongation may reflect the presence of the very strongly bound oxo ligand

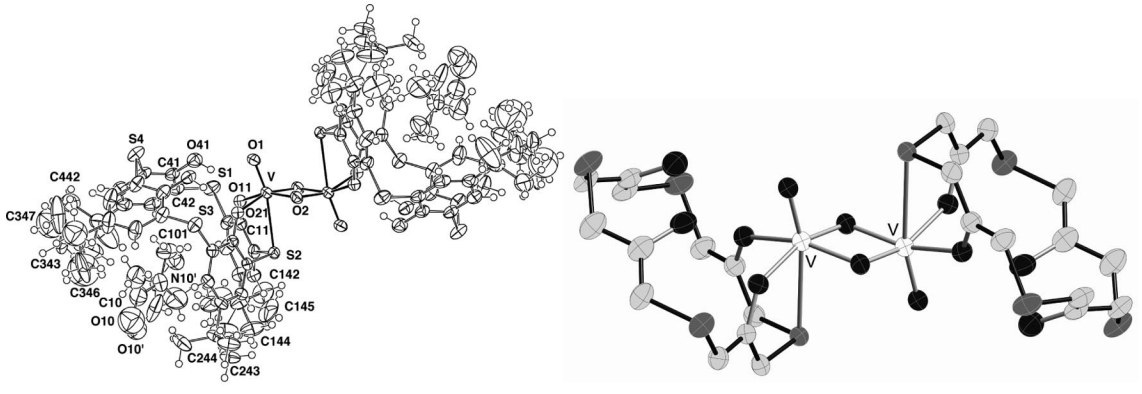

Figure 1. (a) Projection of the centrosymmetric binuclear array of [{(dmf·LH$_2$)$_2$OV(μ-OH)}$_2$](·3dmf·4H$_2$O) (**1**) showing the included dmf. V–O(terminal;bridging) are 1.607(2); 1.806(2), 1.846(2) Å. Within the OSO tripods, V–S;O are 2.7602(8); 1.983(2), 1.978(2) Å. Within the V_2O_2 central rhomb, V···V is 2.7486(10), O···O 2.44(2) Å, O–V–O 82.37(10), V–O–V 97.6(1)°. (b) Simplified, perspective view of the coordination core of the dimer, showing only the macrocyclic ring atoms (and their oxygen substituents) of the calixarene.

trans to the *S*-donor, the strong interaction of the oxygen atom with the vanadium perhaps being a cause of a very reduced basicity, so that the uncoordinated phenolic oxygen atoms come within hydrogen-bonding distances not of this oxygen but only of their adjacent bound phenoxide-*O*.

Within the lattice, the binuclear entities assemble in sheets parallel to the *bc* plane and, as in other examples, these sheets lie one above the other in such a way as to have offset confrontation of the filled calixarene cavities which brings included-dmf-*O* into contact (O···C ≈ 3.5 Å) with CH_3 groups across the interface. The V···V vectors of neighbouring complex units within the sheet are not parallel but intermolecular CH_3···π contacts create regions adjacent to the V_2O_4 cores which are occupied by disordered hydrogen-bonded H_2O-dmf aggregates. There appear to be no hydrogen-bonding contacts of these aggregates to V–OH or VO but a variety of relatively remote dmf-aromatic ring approaches.

$WCl_2(L)\cdot 3.5C_6H_6$ ≡ *cis*-$[Cl_2W(L)](\cdot 3.5C_6H_6)$ (2)

This determination is the most satisfying of the present array (being subject only to minor disorder in one of the lattice solvent molecules), one of the simplest, and also one of the most interesting. All oxygen atoms of the macrocycle are coordinated from the one side of an octahedral six-coordinate mononuclear metal complex, the macrocycle being modelled as a fully deprotonated ligand, with a pair of chlorine atoms disposed "*cis*" completing the array and satisfying charge balance requirements for the W^{VI} oxidation state. The molecule has quasi-2/*m* symmetry. A single molecule, with accompanying lattice solvent molecules, devoid of crystallographic symmetry (one benzene solvent molecule, disposed about a crystallographic inversion centre, excepted), comprises the asymmetric unit of the structure. The conformation of the macrocycle is unusually distorted in this complex (Table S1), though still describable as a grossly pinched *cone*. The tungsten environment (Table S4) is remarkably symmetrical, the two W–Cl distances being closely similar, as are the four W–O distances, despite what must be different *trans*-influences, as well as different interactions with the metal, the interactions described by the associated W–O–C angles being via reflex angles at O(21,41) instead of the more usual, less straight, obtuse angles as found at O(11,31). In consequence, the O_4 array here is unusually non-planar, while the sulfur atoms lie well out of their associated C_6 planes, to the opposite sides to the tungsten atom deviations for rings 1, 3; the associated C–S–C angles are unusually elevated (the largest in the present array of compounds) (Table S2).

The molecular unit (Figure 2) is also unusual in that it is only the third example of a transition-metal complex, after those of U^{VI}[29] and Zr^{IV},[15,30] in which the sulfur atoms of the ligand appear to have no significant role as donors, all W···S distances being >4 Å. We have seen no evidence of any tendency to isomerise, a contrast with complexes of *p*-*tert*-butylcalix[4]arene ($L'H_4$), where both *cis* and *trans* isomers of $WL'Cl_2$ have been characterised.[31] The calixarene conformation is an extreme case where two opposed phenyl rings lie quasi-parallel to the mean S_4 plane ("flattened" orientation) and the other two are quasi-perpendicular to it ("upright") (Table S1). Thus, the "cavity" in this case amounts to a relatively small space between the pair of near-parallel phenyl rings and is not occupied by the benzene component which crystallises with the complex, and lies largely in between the complex units, one molecule at best being described as lying close to the entry to the calixarene cavity, with (disordered) orientations in which there are, amongst others, contacts both to *tert*-butyl CH_3 groups and to phenyl groups (in an "edge-to-face" mode[32]) not of the cavity. A view of the lattice down *c* is particularly useful in providing an understanding of the structure of its complete form. In this view, the WCl_2 groups appear in projection as proximal pairs with opposite orientations of the chloro ligands, a result of the complex units being arrayed in columns, parallel to *c*, in which each unit alternates in orientation but with the more "flattened" phenyl groups of the calixarene remaining essentially in planes perpendicular to the *ab* plane. Between these planes, there are CH_3···π contacts involving the flattened phenyl groups of adjacent columns. Along the columns, the alternating orientations of the complex units allows the "upright" phenyl groups to adopt a slipped stacking array with C···C separations ca. 3.8 Å, once again (as in the Mn^{II} complex below) similar to the situation found in some solvates of the free ligand.[33] The benzene component in the lattice, in the view down *c*, appears to adopt essentially two orientations, one in arrays quasi-perpendicular to *c* aligned parallel to *a*, and the other in columns with the ring planes oriented quasi-parallel to *c*. In fact, the benzene molecules in these two groups interact through "edge-to-face" approaches, as in crystalline benzene itself,[32] as well as interacting (as noted above) with the calixarene units.

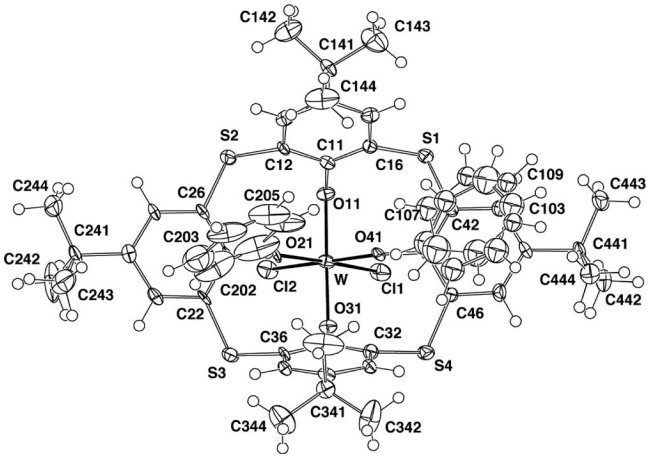

Figure 2. Projection of a single molecule of *cis*-$[Cl_2W(L)](\cdot 3.5C_6H_6)$ (**2**) with the two solvent molecules (one disordered) which approach inclusion. W–Cl are 2.310(1), 2.315(1); W–O 1.884(3)–1.900(2) Å.

$Mn(LH_2)\cdot 3.5CH_2Cl_2$ (×2) ≡ $[\{Mn(H_2L\cdot CH_2Cl_2)\}_2](\cdot 5CH_2Cl_2)$ (3)

The complex molecule (Figure 3) is a neutral, binuclear centrosymmetric array, one half comprising the asymmetric unit of the structure, together with one included and diverse non-included dichloromethane solvent molecules. The molecule has quasi-*2*/*m* symmetry, *2* through the Mn···Mn line, and *m* through the pair of O(312) atoms, but this potential symmetry is broken in the core by the protonic hydrogen dispositions, and at the periphery by substituent orientations. The manganese atom is six-coordinate (Table S5), by two pairs of phenoxide-*O* chelates, derivative of O(21,31) and inversion-generated O(31,41), augmented respectively by the intermediate sulfur atoms S(3,4) so as to form tridentate OS(O-μ) *fac*-tripodal arrays that occupy pairs of opposed *fac* arrays of sites, about the same metal, or, within the same ligand, a pair of sets of tridentate *fac* donors with one atom common ("double tripod") that bridge the pair of metal atoms, the two atoms being constrained by a pair of such ligands, centrosymmetrically related. The sequences O(21),S(3),O(31),S(4),O(41) (and inverse) constrain the metal atoms thus, the S(1),O(11),S(2), sequence not coordinating. Here phenolic hydrogen atoms of the ligand have been located and refined [on O(11,21), directed toward O(41,11) respectively] (Table S1). Mn–O(21) is longer than Mn–O(41), presumably in consequence of O(21) being protonated, O(41) not. O(21)···O(31) is short [2.987(3) Å]. Consideration of the possibility that calixarenes may stabilise metals in high oxidation states[34] led to various efforts to prepare Mn^{III} complexes but the only crystalline species isolated was the present, formulated from its structure determination as above (**3**). The structure of this unit (Figure 3) strongly resembles that of the dimeric In^{III} complex described in the preceding paper.[16] Location of the phenolic hydrogen atoms, however, has confirmed the ligands to be not more than doubly deprotonated, and the bond lengths found (Table S5), as well as the very pale colour of the complex, are typical of Mn^{II}. As it happens, for both M–O and M–S, bond lengths for seven-coordinate In^{III} appear to be very similar to those for six-coordinate Mn^{II}, although, as noted above, Mn–O(21) is long, the phenolic hydrogen atoms H(11,21) both interacting within the O_4 ring [H(11)···O(41) 1.82(4), H(21)···O(11) 1.86(4) Å]. The core M_2O_2/ligand O_4 interplanar dihedral angle here is 53.39(9)°. Solvation differences appear to allow the lattice of the manganese complex to be slightly more compact than that of the indium complex, one reflection of this being that aromatic rings of calixarene ligands in neighbouring complex units come within π-stacking distances, as occurs in solvates of the free ligand.[33,35,36] As in the indium complex, however, filled cavities of the stepped divergent receptor units are in offset confrontation seemingly associated with both CH_3···CH_3 and Cl···CH_3 interactions. The calixarene cavities are again slightly distorted cones, some outward splaying occurring along the mean plane of the CH_2Cl_2 guest. An interesting contrast with the tetrametallic $[Mn_4L_2]$ sandwich species produced by solvothermal synthesis[12] is that here the manganese(II) centres are more nearly octahedral rather than trigonal prismatic as in that case. The origin of this difference is presumably to be associated with the differing degrees of thiacalixarene deproton-

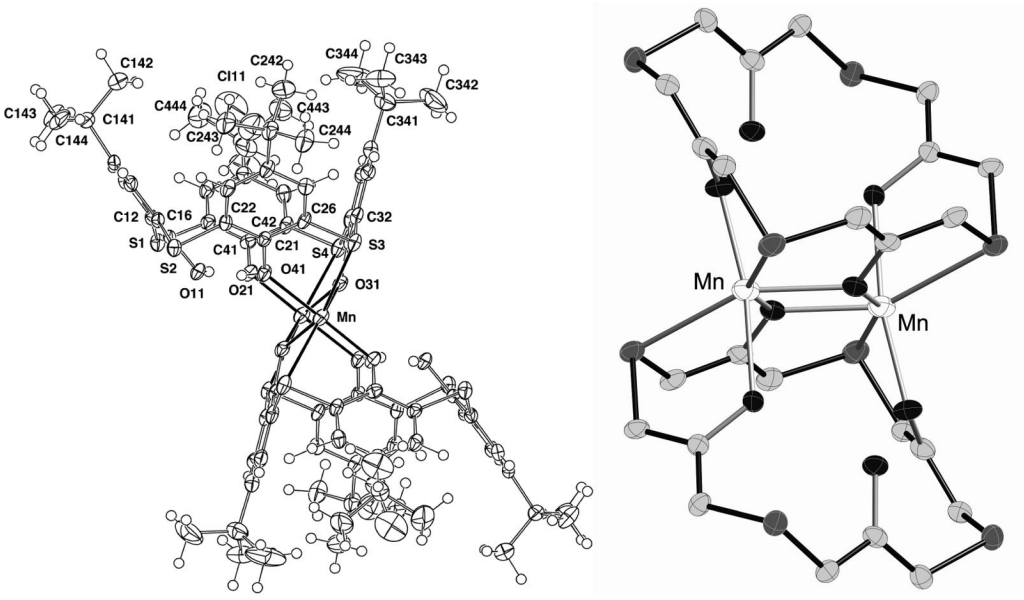

Figure 3. (a) Projection of the centrosymmetric binuclear array of $[\{Mn(H_2L\cdot CH_2Cl_2)\}_2](\cdot 5CH_2Cl_2)$ (**3**) quasi-normal to the ligand axis. Mn–S are 2.679(1), 2.697(1) Å. Mn–O(31)(bridging) are 2.105(2) (×2), Mn–O(phenoxide) 2.213(2), 2.054(2) Å. Within the Mn_2O_2 central rhombs Mn···Mn is 3.256(1), O···O 2.666(5) Å; O–Mn–O 78.6(1), Mn–O–Mn 101.4(1)° [cf. Compound **4a** (Figure 7 of the preceding paper[16])]. (b) Simplified, perspective view of the coordination core of the complex.

ation, though manganese(II) is also found in a distorted trigonal-prismatic environment in a mixed metal derivative of *p-tert*-butylhexathiacalix[6]arene[25] and it may be that its lack of LFSE explains a ready transfer from one geometry to the other.

$Fe_3O(HCO_2)(LH)_2{\cdot}2H_2O{\cdot}6dmf \equiv [OFe\{Fe(OH_2)(\{OCHO\}/\{O\text{-dmf}\})\}_2(HL{\cdot}dmf)_2]({\cdot}2dmf)$ (4)

A thiacalixarene/transition-metal complex (Figure 4) involving an M^{III} species has been obtained here in a crystalline form for the case of M = Fe, although, at least when solvothermal synthesis is utilised, it is also possible to readily obtain polynuclear (tetra- and also decanuclear) Fe^{II} derivatives.[13] All implied protonic hydrogen atoms have been located in the structure determination [on O(131,231) (Table S1)], providing, with one exception, a satisfactory charge balance; the exception arises from the coordination of a pair of unidentate ligands initially ascribed as *O*-dmf, but found to be disorderly, in a manner suggesting 50% formate component (presumed to arise from dmf hydrolysis), thus completing the proposed charge balance. As coordination can activate dmf towards hydrolysis,[37] such reactions might have been expected to complicate many of the syntheses described herein but the problem seems generally rare.[38]

The core of the molecule is the familiar Fe_3O unit,[39] essentially planar with O(0) deviant from the Fe_3 plane by 0.017(2) Å. The usual $\bar{6}m2$ symmetry of this array is degraded to approximate *2m* with significant differences among the Fe···Fe distances and the Fe–O–Fe angles (Table S6, Supporting Information), Fe(2)–O(0) being longer than Fe(1,3)–O(0) which are essentially equal, as are Fe(2)–O(0)–Fe(1,3), cf. Fe(1)–O(0)–Fe(3) which is much larger, concomitantly. The environs of Fe(1,3) are closely similar, and different to that of Fe(2).

The iron atoms Fe(1,3) have six-coordinate, quasi-octahedral coordination geometries (Table S6). Each is associated with one of the two independent macrocycle ligands [each of which is close to a regular *cone* array (Table S1) and has an included dmf] which behaves as an OS(O-μ) *fac*-tridentate/tripod through a pair of adjacent phenoxy-*O* donor O(*l*11,*l*12) [somewhat unsymmetrically bonded (Table S6)], and the intervening sulfur, S(*m*1). The other three coordination sites about each, also necessarily *fac*, comprise the central oxo-*O*, O(0), a water molecule oxygen, O(0*n*), and the mixed unidentate formate/dmf component. One of the phenoxy-*O* donors of each macrocycle, O(*l*11), is also a bridging donor to the central iron atom, Fe(2), forming a further OS(O-μ) *fac*-tridentate array to that atom with the other adjacent phenoxy-*O*, O(*l*21) [the pair of phenolic-*O*-donors now very unsymmetrically bound (Table S6)] and that intervening sulfur S(*m*2), all Fe–O(*l*11) being longer than the Fe–O(*l*21,*l*41). The compact nature of the two tridentate ligands, allowing a Fe(2)···O(0) interaction, raises the coordination number of Fe(2) to seven, all Fe(2)–ligand atom distances thus being concomitantly longer than their counterparts about the six-coordinate peripheral Fe(1,3). The uncoordinated calixarene-O(*l*31) atom is found to be protonated, the hydrogen atom contacting O(*l*41),

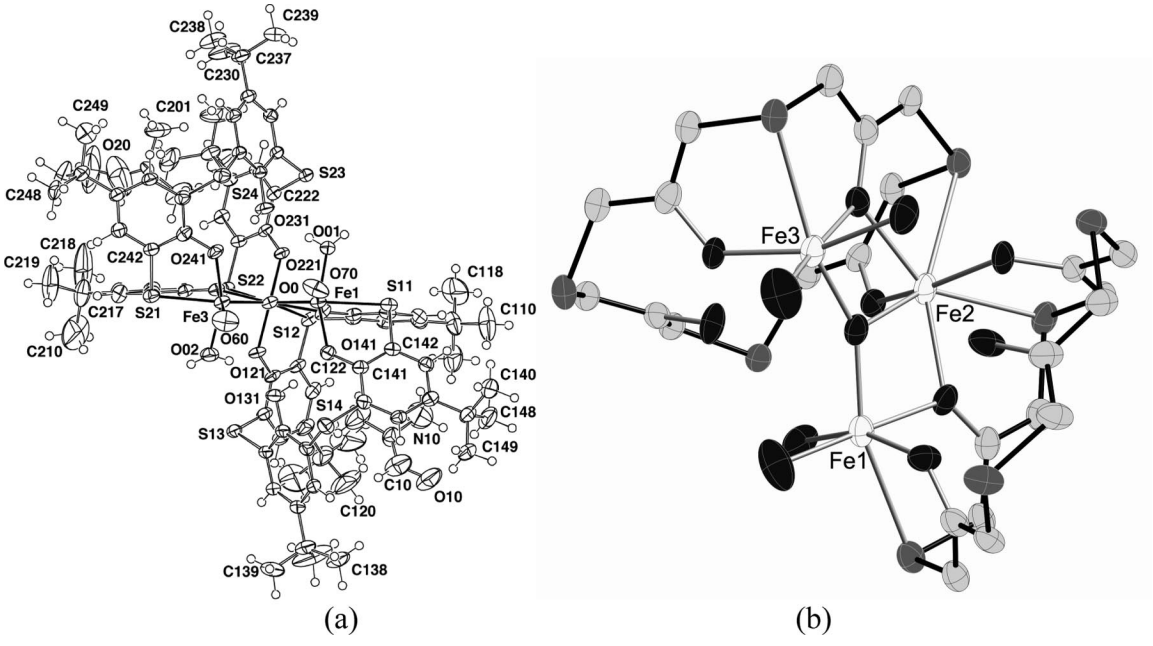

Figure 4. (a) Projection of the trinuclear molecule of $[OFe\{Fe(OH_2)(\{OCHO\}/\{O\text{-dmf}\})\}_2(HL{\cdot}dmf)_2]({\cdot}2dmf)$ (**4**) down the O(0)–Fe(2) line; the disordered (OCHO/dmf) pendant atoms are excluded, for clarity. About the central iron atom [Fe(2)], Fe–O(0) is 2.061(2); within the OSO(μ) tripods, Fe–O(bridging)[O(111,211)] are 2.086(2), 2.122(2) and Fe–O(non-bridging) 1.918(2), 1.916(3) Å. About the peripheral iron atoms [Fe(1,3)], Fe–O(unidentate donor) are 1.975(3), 1.968(3) Å *trans* to O(bridging) and 2.064(2), 2.072(2) Å otherwise. Fe–O(0) are 1.850(2), 1.870(2) Å. Within the OS(O-μ) tripods, Fe–O(μ) are 2.031(2), 2.047(2), and Fe–O 1.968(2), 1.970(2), with Fe–S 2.625(1), 2.617(1) Å. Fe(2)···Fe(1,3) are 3.1729(6), 3.1499(7); Fe(1)···Fe(3) 3.5536(8) Å. Fe(2)–O(0)–Fe(1,3) are 107.5(1), 107.1(1) and Fe(1)–O(0)–Fe(3) 145.5(1)°. (b) Simplified perspective view of the coordination core of the complex.

with the corresponding O(*l*31)···O(*l*41) distance being shorter than the other O···O distances (Table S1). From each coordinated water molecule, one of the hydrogen atoms contacts one or other of the oxygen-component atoms of the disordered lattice dmf 3, the other hydrogen-bonding within the molecule to (phenoxy-) O(*k*131), i.e. of the other ligand. The complex overall can be regarded as a chiral ditopic cavity receptor or twisted connector tecton. Viewed down *a*, the lattice shows columns of complex units parallel to *c*, each column containing homochiral entities but with adjacent columns alternating in chirality. The whole lattice assembly once again displays dmf-filled calixarene cavities in offset confrontation, with close included-dmf-*O*/CH_3 contacts.

The Nickel(II) Complexes of *p-tert*-Butylthiacalix[4]arene (Compounds 5)

Given the ready synthesis and crystallisation of thiacalixarene complexes of Co^{II}, Cu^{II} and Zn^{II}[5a,6] in the form of sandwich species with either three or four metals held between two *cone*-form calices, the behaviour of Ni^{II} was expected to be similar. For reasons which remain obscure, such anticipation proved to be totally unjustified. The finding[4] of a rather different structure for a Zn^{II} complex (of different stoichiometry) should perhaps have served as a warning, but the chemistry of the Ni^{II} system does nevertheless seem to be remarkably complicated. In dmf solutions of $[Ni(dmso)_6](ClO_4)_2$, LH_4 and triethylamine, the colour varies markedly with small change in the metal/ligand ratio, indicating that mixtures of species of very different structure may be present. This may explain why fractional crystallisation of the product of such a reaction when the initial ratio was 2:1 provided several species in addition to only one structurally characterisable component. Kinetic factors, also, were clearly important. Thus, in one such synthesis, the total product, isolated by extraction into dichloromethane, could be concentrated to give a green-yellow powder which readily redissolved in dichloromethane. In a duplicate experiment, this residue proved to be seemingly completely insoluble in dichloromethane, as well as in boiling dmf and boiling toluene, though when left to stand under a cooling mixture of dmf and toluene, it dissolved completely in fifteen minutes! It is, of course, well-recognised that elaboration of all the factors leading to polynuclear complexes (such as formed by thiacalixarenes) is exceedingly difficult.[40] The properties of mixtures derived from the perchlorate, nitrate, acetate, chloride and bromide were all completely different (even though the structurally characterised complex **5a** obtained from $NiCl_2$ contains no chloride). This may be due to "anion templating", a well-recognised factor in synthesis,[41] even if it is usually manifested in the presence of the anion in the product.

$(Et_3NH)Ni_2(LH)(LH_2)\cdot 2dmf\cdot 2(CH_3)_2CO\cdot H_2O \equiv (Et_3NH)[Ni_2(LH_2\cdot Me_2CO)(LH\cdot dmf)]\cdot dmf\cdot Me_2CO\cdot H_2O$ (5a)

Refinement of the phenolic hydrogen atoms establishes the nature of the cation/anion component of the structure beyond reasonable doubt. Binuclear and with a pair of associated thiacalixarene ligands like the Mn^{II} complex, **3**, the ligand protonation now differs, so that the complex species is anionic rather than neutral. The present array is devoid

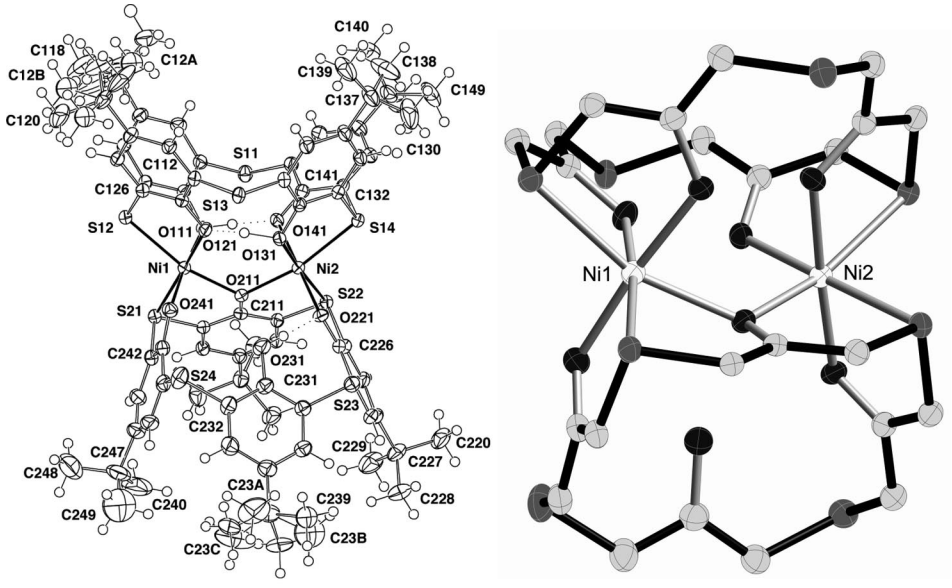

(a) (b)

Figure 5. (a) A projection of the binuclear $[Ni_2(LH_2\cdot Me_2CO)(LH\cdot dmf)]$ array of **5a**. Ni(1)–S(12),Ni(2)–S(14) are 2.4274(8), 2.4358(7); Ni(1)–S(21), Ni(2)–S(22) are 2.3768(8), 2.3693(7) Å. Ni(1,2)–O(211) are 2.092(2), 2.084(2); Ni(1)–O(241), Ni(2)–O(221) are 1.991(2), 1.982(2); Ni(1)–O(111), Ni(2)–O(131) are 2.079(2), 2.058(2) and Ni(1)–O(121), Ni(2)–O(141) are 2.025(2), 2.038(2) Å. Ni(1)···Ni(2) is 3.6374(5) Å. Ni(1)–O(211)–Ni(2) is 121.19(9)°. Ligand 1 contains the (disordered) acetone. (b) The coordination core of the complex.

of crystallographic symmetry, one formula unit (Figure 5) being the asymmetric unit of the structure; the anion array has *quasi-2* symmetry, but the proton distribution within ligand 2 violates this. Ligand 1 includes a disordered acetone molecule, ligand 2 a dmf molecule.

The two nickel atoms are linked directly by a single phenoxide oxygen atom, O(211), from ligand 2, with the Ni–O–Ni angle 121.19(9)°, Ni···Ni 3.6374(5) Å. The coordination environments of both nickel atoms are NiS_2O_4, with the pair of sulfur atoms *cis*; there is a disparity between the Ni–S distances, the longer being *trans* to the bridging oxygen atom, that Ni–O distance in each case being the longest Ni–O distance in each coordination sphere (Table S7, Supporting Information). In ligand 1, the phenolic hydrogen atoms on O(111,131) were clearly located and refined; they hydrogen bond to O(141,121) respectively: O,H(111)···O(141) 2.400(3), 1.48(5); O,H(131)···O(121) 2.395(3), 1.14(6) Å. The ligand bonds as a pair of *fac* (H)OSO tripods, one to each nickel atom, with the concomitant that the angles at the central, tripodal sulfur atoms (98.8(1), 100.0(1)° are appreciably less than those at the "stretched", non-coordinated atoms [108.7(1), 107.0(1)°] (Table S7, Supporting Information); the chelating O···O distances [3.012(3), 2.979(3) Å] are much longer than the hydrogen-bonded distances between adjacent oxygen atoms in the ligand (Table S1), while the Ni–O distances to the protonated phenolic oxygen atoms [2.079(2), 2.058(2) Å] are longer than those to the non-protonated [2.025(2), 2.038(2) Å].

In projection down the axis through ligand 1, the relative orientation of ligand 2 is "staggered", albeit unsymmetrically, since one of the phenolic oxygen atoms – O(231) (which is protonated) – does not coordinate; whereas in ligand 1, the pair of uncoordinated sulfur atoms are opposed in the macrocycle, here the pair are those to either side of O(231), i.e. S(23,24), with associated C–S–C angles closely akin to those at the coordinated [range, C–S–C (ligand 2) 101.6(1)–103.9(1)°]. The ligand coordinates as a pair of *fac*-OS(O-μ) tripods, but now with O(211) common to both tripods; the Ni–O distances to the other unprotonated oxygen atom of each tripod [1.991(2), 1.982(2) Å] are the shortest in the coordination sphere. O(211)···O(221,241), the chelate distances, are 3.046(3), 3.016(3) Å, cf. O(231)···O(221,241) 2.639(3), 3.382(3), the former being associated with the hydrogen-bond H(231)···O(221) 1.78(5) Å. The asymmetry of ligand 2 is seen in the interplanar dihedral angles (Table S1).

$Ni_6(L)(LH)_2(LH_2)\cdot 4MeCN\cdot 6H_2O \equiv [\{Ni_4(H_2O)(L\cdot MeCN)(LH\cdot MeCN)\}\{Ni_2(LH\cdot MeCN)(LH_2\cdot MeCN)\}]\cdot 5H_2O$ (5b)

Here again, the full formula unit, devoid of crystallographic symmetry, comprises the asymmetric unit of the structure. Although the second relatively simple complex structurally characterised for Ni^{II} has the same stoichiometry, M_3L_2, as the Co^{II} and Zn^{II} complexes obtained in analogous syntheses,[6] it in fact is a combination of a tetranuclear and a binuclear array, each encompassed by two ligands, with an Ni–S bond linking the two (Figure 6). Each of the ligand cavities includes an acetonitrile molecule. Phenolic hydrogen atoms were not located or refined and were assigned on geometrical considerations.

The binuclear array [comprising Ni(5,6) and ligands 3,4] is very similar to that of **5a**. Ligand 4 provides a pair of O_2S *fac*-tripods opposed in the macrocycle, differing from **5a** in that the protonation assignment is such that the pair of protonated phenolic oxygen atoms are located in the one tripod. In ligand 3, as in **5a**, the pair of OS(O-μ) tripods are adjacent in the macrocycle, by virtue of the common oxygen atom bridging the two nickel atoms, with a further $S_2O(H)$ tripod, embracing the protonated oxygen atom, being uncoordinated. The nickel atom environments again are *cis*-S_2O_4, made up of pairs of tripods, one of the form OS(O-μ) from ligand 3, and the other OSO, from ligand 4, "staggered", with respect to ligand 3.

The second cluster – of four nickel atoms and two ligands – is unusual. Aggregates of four metal atoms and two thiacalixarene ligands have been characterised in highly symmetrical, "sandwich" forms for Cu^{II},[5a] Hg^{II}[8] (both revisited presently ahead) and Nd^{III}.[7] Such an array is also found in the lead(II) and lanthanide(III) oxo complexes reported in the previous[16] and following[17] papers. The ligands are "eclipsed" with respect to each other, and the (approximate) gross symmetry 4/*mmm*. In the copper and mercury arrays, with "small" and "large" metal atoms, both prone to low-symmetry coordination environments, the ligands are fully deprotonated. In the present array, the Ni_4 grouping is "quasi-planar", atom deviations δNi(1–4) being 0.115(1), –0.143(1), 0.177(1), –0.149(1) Å, the two ligands lying above and below the "plane" as usual. The Ni_4 unit is not square but trapezoidal, Ni(1)···Ni(4), Ni(2)···Ni(3), Ni(3)···Ni(4) being 3.2778(4), 3.006(2), 3.1063(4) Å, while Ni(1)···Ni(2) is 3.6198(4) Å. The diagonals, Ni(1)···Ni(3), Ni(2)···Ni(4), are grossly disparate: 3.4753(4), 5.4348(4) Å. Notwithstanding, ligand 1, fully deprotonated, is poised above the "plane" of the four nickel atoms with the phenoxide oxygen atoms bridging pairs of nickel atoms, and the sulfur atoms coordinating to their counterpart nickel atoms, so that each nickel atom is coordinated by a $S(\mu\text{-}O)_2$ tripod. Irregularities are found among the other associated structural parameters (Tables S1, S8): Ni–S range between 2.3611(6)–3.2540(6) Å and Ni-(μ-O) between 1.963(1)–2.102(1) Å, the latter (longest) distance being associated with the long [3.6198(4) Å] edge of the Ni_4 "square". The (remarkably) long Ni–S distance [3.2540(6) Å], Ni(3)···S(13), is associated with a nickel atom environment in which the angular geometries are far from orthogonal, and this nickel atom, unlike the other three, may perhaps more properly be considered five- rather than six- coordinate. These perturbations are reflected in other ligand parameters (Table S1).

The distortions in the Ni_4 array reflect the disposition and binding of ligand 2 on the other side of the plane. Here O(231) bridges Ni(2,3), with S(23,24) binding to either side to Ni(2,3). O(241) not only bridges Ni(3,4) but also forms

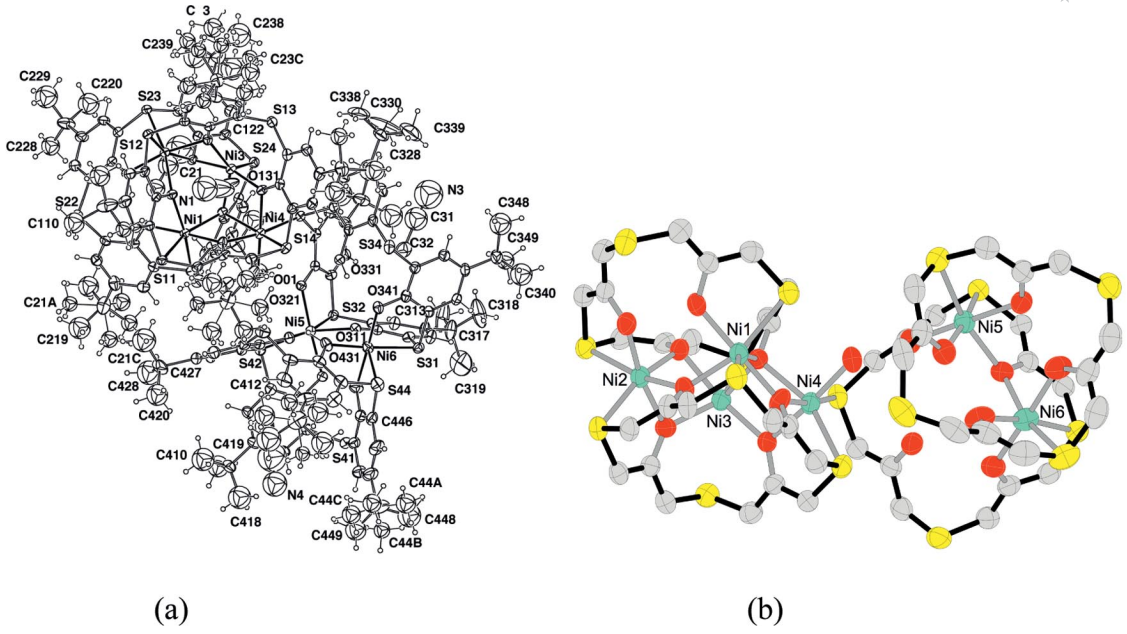

Figure 6. (a) The aggregate of [{$Ni_4(H_2O)$(L·MeCN)(LH·MeCN)}{Ni_2(LH·MeCN)(LH_2·MeCN)}](·5H_2O) (**5b**), projected (approximately) down the axis of the Ni_4L_2 component and normal to the axis of the Ni_2L_2 component. In the latter, Ni(5)–S(42), Ni(6)–S(44) are 2.4749(7), 2.4590(7); Ni(5)–S(32), Ni(6)–S(31) are 2.3853(7), 2.3599(8) Å. Ni(5,6)–O(311) are 2.094(1), 2.092(1), Ni(5)–O(321), Ni(6)–O(341) are 2.014(1), 1.984(1), Ni(1)–O(421), Ni(2)–O(441) are 2.053(2), 2.076(2) and Ni(5)–O(411), Ni(6)–O(431) 2.061(1), 2.031(2) Å. Ni(5)···Ni(6) is 3.6538(4) Å. [All to be compared with the data of Figure 5, (a)]. In the tetranuclear component, regarding ligand 1, Ni(1)–S(11), Ni(2)–S(12), Ni(3)–S(13), Ni(4)–S(14) are 2.4592(7), 2.3611(6), 3.2540(6), 2.3944(7) with Ni(1,2)–O(111) 2.036(1), 2.102(1); Ni(2,3)–O(121) 2.038(1), 1.996(1), Ni(3,4)–O(131) 2.010(1), 2.005(1); Ni(1,4)–O(141) 1.963(1), 1.969(2) Å. Regarding the ligand 2, Ni(1)–S(21), Ni(2)–S(23), Ni(3)–S(24) are 2.4786(6), 2.4539(6), 2.4457(7); [Ni(4)–S(33) is 2.4661(7) Å]. Ni(1)–O(211) is 2.041(2), Ni(2,3)–O(221,231) 2.027(1), 2.060(1), Ni(1,3,4)–O(241) 2.187(2), 2.007(1), 2.181(1) Å. Ni(4)–O(water) is 2.002(1) Å. Ni(1)···Ni(2,3,4) are 3.6198(4), 3.4753(4), 3.2778(4); Ni(2)···Ni(3,4) are 3.0062(4), 5.4348(4); Ni(3)···Ni(4) is 3.1063(4) Å. (b) A simplified, perspective view of the coordination core, centred on the S atom bridging the Ni_2 and Ni_6 units (C = grey, O = red, S = yellow, Ni = green).

a triple bridge to Ni(1), the distances O(241)–Ni(1,4) being rather long at 2.186(2), 2.181(1) Å. Thus, S(21) is now appropriately disposed to bind not to Ni(4) but to Ni(1), the lack of accessible sulfur and a bridging oxygen atom at Ni(4) being made up by coordination of S(33) from the binuclear array, and an oxygen atom O(01) from a water molecule. Between Ni(1) and Ni(2), O(211) and O(221) bind as unidentate, not bridging, donors with S(22), in between, uncoordinated, the gross effect being an offset of the O_4 "face" of the ligand with respect to the Ni_4 array. The considerable perturbations of the ligand symmetry from 4*m* are summarised in Table S1, Supporting Information.

Elemental analysis of some of the amorphous material (confirmed to be so by powder diffractometry) obtained along with the crystalline hexa-nickel species described above provided a good fit to the stoichiometry $Ni_6L_2(dmf)_4(OH)_4$ [$C_{92}H_{120}N_4Ni_6O_{16}S_8$ (2146.7): calcd. C 51.47, H 5.63, N 2.61, S 11.95; found C 51.6, H 5.7, N 2.7, S 11.4], indicating that other components present may have been precursors to the following Ni_{32} complex **5c** crystallised under different conditions. The formation of this large hydrolytic oligomer **5c** appears to require an extended period of reaction (weeks) at room temperature, though it is unclear as to what extent this may be determined by the rate of crystal deposition.

$Ni_{32}(OH)_{40}(L)_6$·8dmso·10dmf ≡ [$Ni_{32}(OH)_{40}(L)_6$]·8dmso·10dmf (5c)

This unusually high nuclearity species, Figure 7, (a), has a topology identical to that of the nickel atoms in the cluster of [$MePPh_3$][$Ni_{32}C_6(CO)_{36}$]·MeCN,[42] though quite unlike that of a hydrolytic Ga_{32} array.[43] The structure is closely related to that of the recently reported[44] Co_{32}(thiacalix[4]arene)$_6$ complex, although that appears to contain both Co^{II} and Co^{III} centres, whereas the present complex appears to contain only Ni^{II}. The Co complex was prepared by a solvothermal method (at 130 °C), which has the obvious advantage of rapid kinetics compared to the procedure we have used to obtain the Ni complex but this may also have led to the partial oxidation and extensive hydrolysis, explaining why a much simpler true Co^{II} complex was obtained in our earlier work.[6] Of potentially high intrinsic symmetry, the complex molecule **5c** is disposed about a crystallographic inversion centre, so that one half of the formula unit comprises the asymmetric unit of the structure; the solvent component of the structure, modelled in terms of dmso and dmf is not closely associated with the neutral aggregate, either by inclusion or coordination, and simply represents the better defined component of lattice voids. The metallic component of the structure comprises a quasi-

spherical shell made up of two sets of nickel atoms. One set [hexagons in the schematics of Figure 7, (b,c)] of twenty-four [Ni(5–16) and inverses], is disposed at the vertices of a cuboctahedron; the other set (squares in the schematics) of eight [Ni(1–4) and inverses], comprises a cube, the vertices of which lie close to the centroids of the eight hexagonal faces of the cuboctahedron, slightly displaced "inwards" toward the inversion centre and with edge lengths closely ranged [< > 4.26(3) Å; Figure 7, (b), Table 1 and Table S9]; distances to the nearest cuboctahedral nickel atoms are (< >) 3.261(14) Å. Although "equivalent" parameters of the structure are mostly very closely ranged (Table 1), the hexagonal faces of the cuboctahedron are not exactly regular: the three edges that adjoin other hexagonal faces are shorter [(< >) 3.029(12) Å] than the distances in the square faces (< >) 3.449(15) Å; nonetheless, the angles in the hexagonal faces range closely from 119.25(5) to 120.49(5)°, and in the square faces from 89.11(5) to 90.62(5)°.

Of the "hydroxy" components of the cluster, one set of sixteen lies within the shell of nickel atoms, towards the inversion centre, with the other set of twenty-four [oxygen components O(01–012) and images] without. In projection, the latter lie within the hexagonal faces of the cuboctahedron, each bridging the central "cuboidal" nickel atom to a pair of cuboctahedral nickel atoms on a hexagon/hexagon edge [Figure 7, (c)(i)]. The Ni–O distance associated with the former (thick lines in the Figure) is appreciably shorter [< > 1.984(13) Å] than the (equivalent) latter pair [< >, 2.043(15) Å] (thin lines in the Figure); the angle between the latter pair is appreciably smaller [< >, 95.7(7)°] than

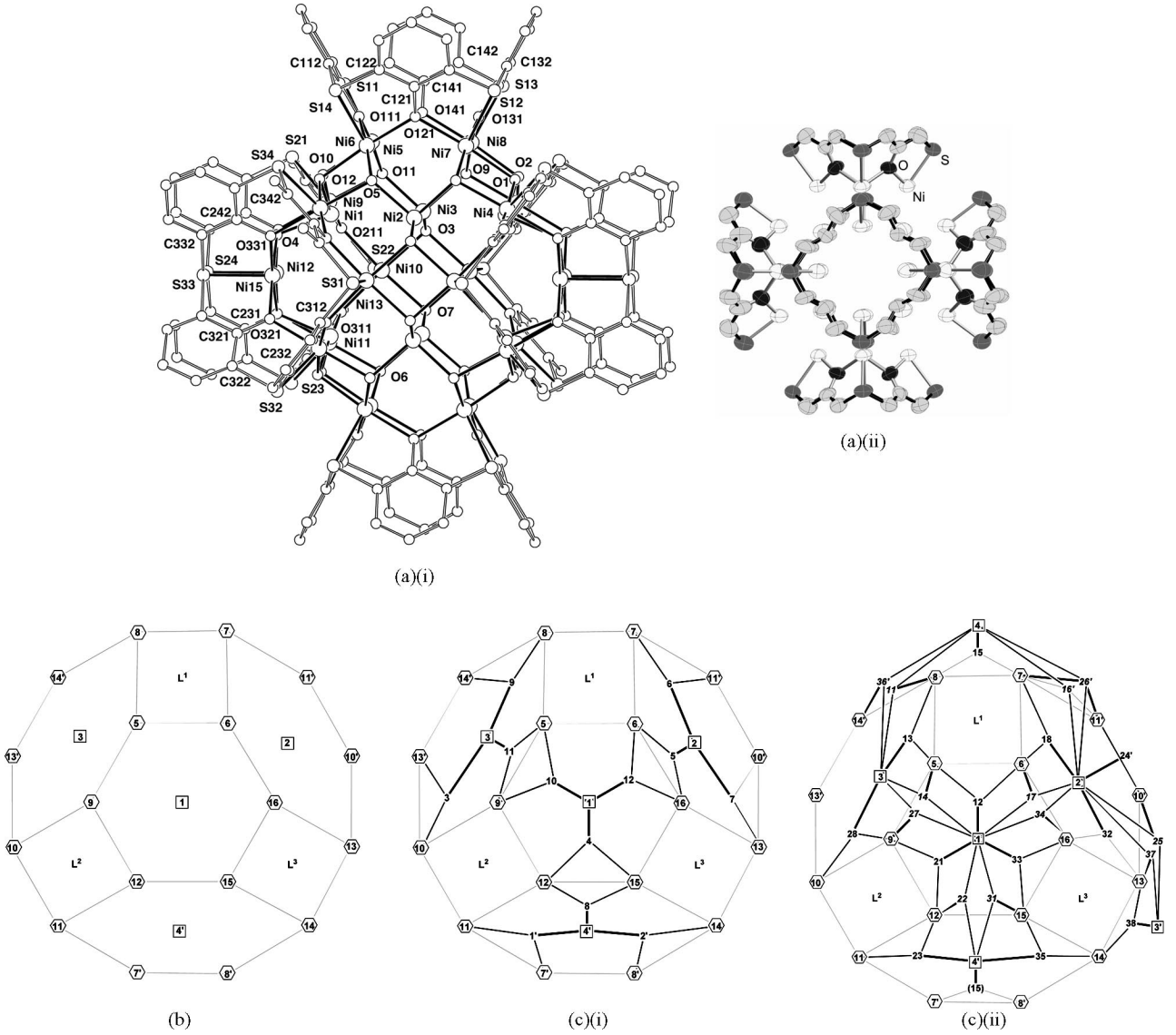

Figure 7. Projection of the oligonuclear array of $[Ni_{32}(OH)_{40}(L)_6]$(·8dmso·10dmf) (**5c**): (a)(i) down a quasi-2 axis (*tert*-butyl groups omitted for clarity); (a)(ii) simplified perspective view, down a 4-axis, of the coordination core with OH groups omitted. (b) Schematic showing the cuboctahedral Ni_{24} array with the Ni_8 cube set at the centres of the hexagonal faces. (c) Schematic of the hydroxy group connectivities of the groups (c)(i) external; (c)(ii) internal to the nickel cluster. Oxygen atoms in the former [O(*mn*)] and in the latter [O(0*mn*)] are denoted *mn*; primed atoms are inversion-related.

Table 1. Summary of $[Ni_{32}(OH)_{40}(L)_6]$ parameters in **5c**. A full tabulation is given Tables S9.1 and 9.2 (Supporting Information). Primed atoms are inversion related.

(a) Parameters associated with the $(Ni_4)_2$ cube, Ni(1–4, 1′-4′).	
<Ni···Ni> (cube edges)	4.26(3) Å
<Ni–O(H)(external)>	1.982(13) Å
<Ni–O(H)(internal; fragments)>	2.34(4) Å
<(H)O(external)–Ni–O(H)(external)	94.5(10)°
<(H)O(external)–Ni–O(H)(internal; fragments)>	173.7(10), 155.8(11)°
<O(internal)···O(internal)> (interfragment)	1.87(6), 1.07(4) Å
<O(internal)–Ni–O(internal)> (interfragment)	46.7(16), 26.6(12)°
Ni(cube)···Ni(cuboctahedron)	3.261(14) Å
(b) Parameters associated with the $(Ni_{12})_2$ cuboctahedron, Ni(5–16, 5′-16′).	
<Ni···Ni>	3.029(12), 3.449(15), 4.878(16) Å
Ni···Ni···Ni (hexagonal faces)	119.23(6)–120.49(5)°
Ni···Ni···Ni (square faces)	89.11(5)–90.62(5) Å
<Ni···S>	2.418(15) Å
Ni–O(thiacalix)	2.013(14) Å
Ni–O(H)(external)	2.043(15) Å
Ni–O(H)(internal, fragment)	2.17(3), 2.31(4) Å
<S–Ni–O(thiacalix)>	84.3(4)°
S–Ni–O(H)(external)	99.6(7)°
<S–Ni–O(H)(internal, fragment)>	174.3(10), 156.5(7)°
<O(thiacalix)–Ni–O(thiacalix)>	92.4(8)°
<O(thiacalix)–Ni–O(H)(external)>	174.5(7), 91.8(8)°
<(H)O(external)–Ni–O(H)(external)>	83.7(6)°
<(H)O···O(H)> interfragment distances	1.39(6), 1.07(4) Å
<(H)O–Ni–O(H)> interfragment angles	35.3(16), 27.4(12)°

the other pair of (equivalent) angles [< >, 108.2(11)°]. These "outer", "*fac*", $(\mu_3\text{-}OH)_3$ faces of the coordination environments of the "cuboidal" nickel atoms have "equivalent" associated Ni–O distances of [< > 1.984(13) Å]. Dmso oxygen atoms show approaches as a "second coordination sphere" to triads of the external hydrogen atoms of the hydroxy group: H(4,10,12) to O(101), H(5,6,7) to O(20), H(3,9,11) to O(30), H(1,2,8) to O(40) [<O···O> 2.83(8); <H···O> 2.01(11) Å]. The internal component comprises [Figure 7, (c)(ii)] disordered fragments [O(013–036) and inverses] each assigned as one-third of an hydroxy-oxygen atom; the associated hydrogen-atom location is obscure and may or may not be disordered. The twenty-four independent fragments may be divided into two sets of twelve. One set [O(011, 014, 016, 017, 022, 025, 026, 027, 031, 034, 036, 037)] (italicised in the figure) is most closely associated, one-to-one with the set of cuboctahedral nickel atoms (thick bonds), and lie *trans* to the single sulfur atom which lies within each coordination sphere. The other set of twelve fragments ($12 \times 1/3 = 4$) are most closely associated (thin bonds) (a) with the cubanoid set of nickel atoms, lying *trans*, one-to-one, with the oxygen atoms of the exterior hydroxy set, each nickel atom associated with three of the latter and three corresponding internal fragments, with O(int)–Ni–O(int) (< >) 102.6(10)°; (b) with two cuboctahedral nickel atoms at a similar distance [< > 2.30(4), cf. 2.32(4) Å]. The nickel and hydroxy component of the aggregate may thus be represented as $\{Ni_4Ni_{12}(OH)_8(OH)_{12}\}_2$.

The six tetra-anionic thiacalixarene ligands are associated with the six square faces of the cuboctahedral nickel array, one sulfur atom per nickel atom with the two phenolic oxygen atoms of the aromatic rings to either side bridging at the midpoints between the parent nickel atom and those to either side, so that the (μ-O)S(O-μ) combination is once again a (*fac*) tripod about the parent nickel atom. The putative symmetry of the $[\{Ni_{16}(OH)_{20}(L_3)_2\}_2]$ array is 4/*mmm*. The thiacalixarene units can be considered to provide a lipophilic sheath enveloping the hydrolytic cluster.

$2Cuac_2{\cdot}Cu_2(L){\cdot}dmf{\cdot}4.5CH_2Cl_2$ ≡ [(ac-*O*,*O*′-μ)$_4$(dmf-*O*)-$Cu_4(L{\cdot}H_2CCl_2)$]($\cdot 3.5CH_2Cl_2$) (6) (ac = acetate)

In contrast to the Ni^{II} complexes, those of Cu^{II} are very readily isolated and crystallised. Here, divergence from the motif of a metal cluster held between at least two calixarenes, first structurally characterised in $[Cu_4(L{\cdot}CH_2Cl_2)_2]$-$(\cdot CH_2Cl_2)$[5a] but now known for many species[1,2,28] including main group metals,[16,35] is readily observed by means of a synthesis in which the ratio of copper(II) (as the acetate) to the ligand is changed from 2:1 to 4:1. This provides an "open sandwich" structure in the complex **6**, although its magnetic properties (antiferromagnetic coupling, θ –111°) are virtually identical to those of the true sandwich species. Complete deprotonation of both acetate and thiacalixarene ligands provides a neutral tetranuclear molecule, with one dichloromethane molecule included in the macrocycle cavity along with others in the lattice, and a single dmf molecule being apparently symmetrically bound to all four copper atoms; one half of the aggregate comprises the asymmetric unit of the structure, a crystallographic mirror plane passing through Cu(1,3)S(1,3), the chlorine atoms of the included solvent, and the oxygen of the dmf, and bisec-

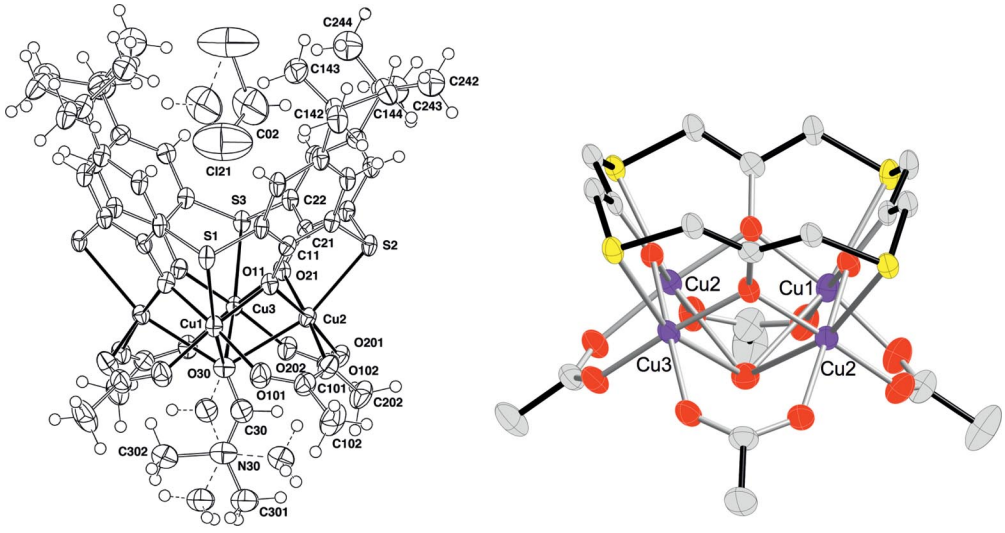

Figure 8. (a) Projection of the tetranuclear array of [(ac-*O*,*O*′-μ)$_4$(dmf-*O*)Cu$_4$(L·H$_2$CCl$_2$)](·3.5CH$_2$Cl$_2$) (**6**) normal to the axis of the macrocycle. The array is of *m* symmetry, *m* through Cu(1,3), S(1,3) of the included dichloromethane (disordered) and O(30) of the dmf (pendent atoms also disordered, about the mirror plane). Regarding the S(μ-O)$_2$ tripods, Cu(1)–S(1), Cu(3)–S(3) are 2.627(3), 2.660(2); Cu(1)–O(11), Cu(3)–O(21) are 1.943(3), 1.956(2); Cu(2)–O(11,21) are 1.945(3), 1.958(3) Å. Regarding the acetates, Cu(2)–O(102,201) are 1.955(3), 1.948(3), Cu(1)–O(101), Cu(3)–O(202) 1.946(3) Å (×2). Regarding the dmfs, Cu(1)–O(30), Cu(2)–O(30), Cu(3)–O(3) are 2.646(5), 2.648(2), 2.605(5) Å. Cu(2)···Cu(1,3) are 3.1715(7), 3.1683(7) Å. (b) Simplified, perspective view of the coordination core (C = grey, O = red, S = yellow, Cu = violet).

ting the macrocycle ligand (Figure 8, Table S10). The Cu$_4$ and O$_4$ arrays form obligate planes, the former fused by the latter atoms bridging above the Cu$_4$ plane, and by the *O*,*O*′-acetate groupings, which link them below the plane. The dihedral angles of the C$_2$O$_2$ acetate planes from the Cu$_4$ plane are 33.1(2), 37.7(2)°, with copper atom deviations of 0.262(8), 0.126(8) Å [Cu(1,2) from ac(1)] and 0.054(7), 0.073(7) Å [Cu(2,3) from ac(2)]. The copper atom environments are six-coordinate (Table S10), but with the quasi-octahedral geometries being grossly distorted towards a "square-planar" form comprised of *cis*-pairs of acetate and macrocycle oxygen atoms, the more distant *trans*-fifth and sixth sites being filled by (a) the μ$_4$-dmf-oxygen atom, common to all four copper atoms as a molecular apex, and (b) the four sulfur atoms on a 1:1 basis. The Cu$_4$ grouping is close to a square array (Table S10, Supporting Information).

The unusual coordination mode for dmf is presumably part of the reason why it is not found included within the calixarene. Viewed down *a*, the complex units appear to form undulating columns parallel to that axis, with the undulation or tilting of one unit relative to another being such that the Cu$_4$ squares project as pairs where a corner of one lies over the centre of the next. There is a partial confrontation of a filled cavity with the acetate/dmf "base" of the next complex unit but any contacts seem to be largely mediated by intervening dichloromethane molecules. Between molecules in adjacent columns, there are CH$_3$···CH$_3$ and CH$_3$···π contacts ca. 3.8 Å.

CaPd$_2$(LH)$_2$·1.5CH$_2$Cl$_2$ ≡ [Ca{Pd(HL)}$_2$](·1.5CH$_2$Cl$_2$) (7a)

Another unexpected feature of thiacalixarene coordination by transition metals is the apparent affinity of the Pd^{II} complex[10] for Ca^{II}, leading to the formation of several mixed-metal species, to date largely explored only in the chemistry of thiacalix[4]arene derivatives.[3d,45] Though discovered by accident, the probable cause being the presence of gypsum in chromatographic media, mixed Pd/Ca complexes can be prepared deliberately by adding Ca^{II} to the reaction medium, resulting in a series of species with Pd/Ca ratios of 2:1, 1:1 and 1:2. After the tungsten complex, **2**, these complexes are the first in the present series of studies to exhibit marked deviations of the calixarene conformation from fourfold symmetry, an effect which is presumably to be associated with Pd^{II} coordination, since, as noted previously,[16] coordination to Ca^{II} alone does not produce a significant change, though it is also true that the distortions in the simple Pd^{II} complex [Pd$_2$(H$_2$L·CH$_3$CN)$_2$] are slight.[10]

The uncertainties concerning the central atom in the beautiful structure **7a** are detailed in the Experimental Section below; with that reservation, the results of the X-ray study define a novel neutral hetero-trinuclear array. One formula unit (together with lattice solvent molecules, none of which are included), devoid of crystallographic symmetry, comprises the asymmetric unit of the structure; the array has putative 2-symmetry [Figure 9, Table S11, (a)].

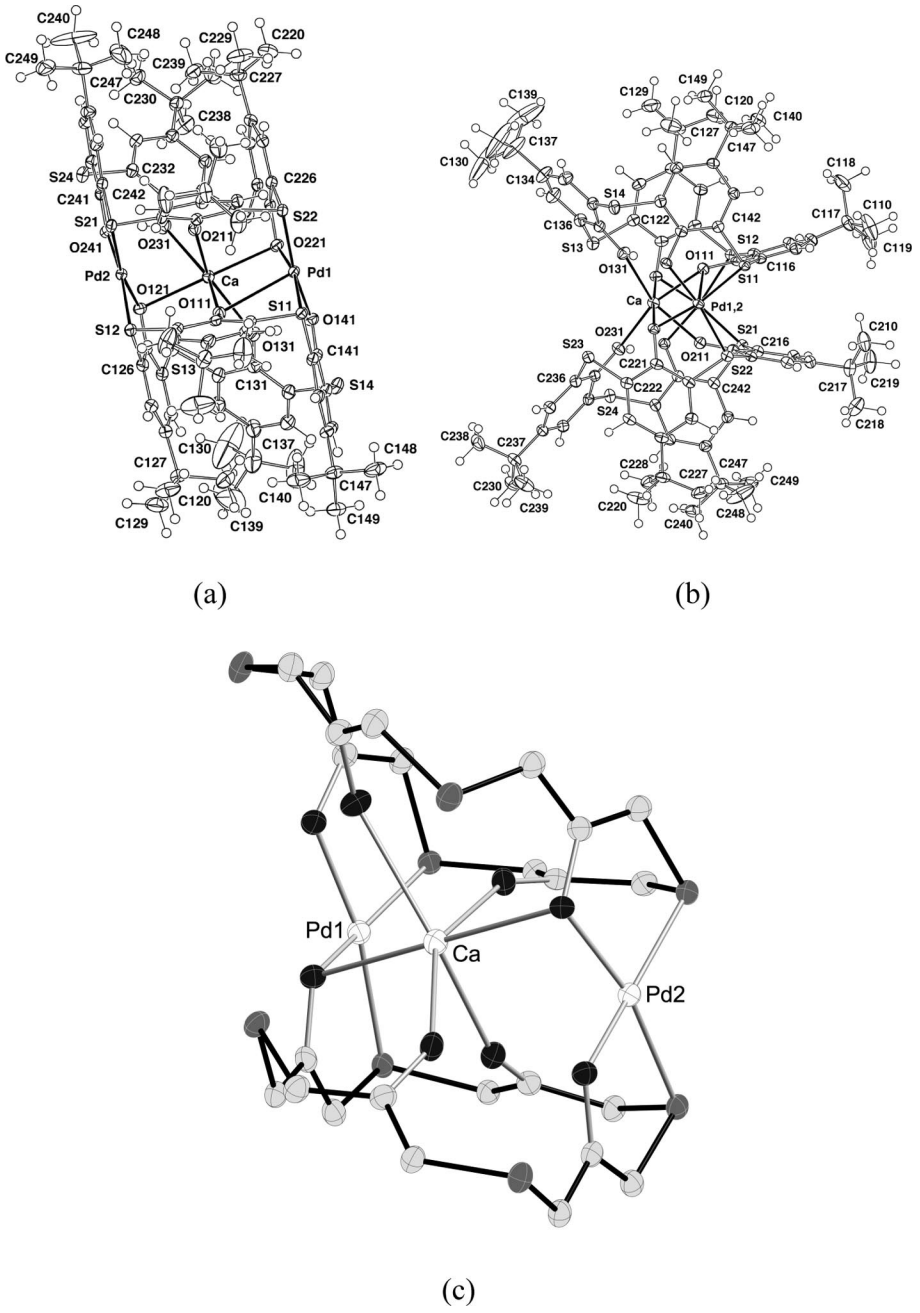

Figure 9. Projections of the heterotrinuclear array of $[Ca\{Pd(HL)\}_2](\cdot 1.5CH_2Cl_2)$ (**7a**): (a) down its quasi-2 axis; (b) approximately down the Pd(1)···Pd(2) line. About the Pd atoms, Pd–S are 2.2549(8), 2.2678(7), Pd–O 2.009(2)–2.016(2) Å; about the calcium Ca–O(111,211) are 2.306(2), 2.338(2); Ca–O(121,221) 2.448(2), 2.446(2), and Ca–O(131,231) 2.596(2), 2.593(3) Å. Ca···Pd(1,2) are 3.2909(7), 3.2579(6) Å. (c) Simplified, perspective view of the coordination core.

In the structure of **7a**, rings 2 and 4 of each ligand lie quasi-parallel but do not overlap exactly in the direction of the macrocycle axis. Within each ligand O(l21), S(l2) and O(l41), S(l4) form pairs of chelates which between them, coordinate a pair of palladium atoms, both in "square-planar" coordination environments, and so that the rings 14/22 and 12/24 are quasi-coplanar, together with the palladium atoms [interplanar dihedral angles 17.2(1), 19.3(1)°] (Table S1), bounding the molecule by a pair of flat "sheets" (Figure 9). Each PdO_2S_2 array is *cis*. Within each ligand, O(l11,l21,l31) are oriented as triads with the capability to coordinate bis(*fac*) about each six-coordinate calcium, with distances increasing in the order O (terminally coordinated to palladium), O (bridging to palladium) and O (protonated, feebly interacting). Whereas Figure 9, (a) conveys the impression that Pd(1)CaPd(2) are collinear, Figure 9, (b) shows that the calcium atom is rather exposed, with a large O(131)–Ca–O(231) angle [123.52(8)°]. The geometry about

Ca is well-removed from octahedral, one *trans*-angle being 177.29(9)°, but the others, involving O(131,231), only 150.79(9), 150.98(8)°.

In **7a**, the calixarene ligands provide all of the donor atoms for both the palladium and calcium centres. If it is true that Pd^{II} can strongly modify the ligand conformation, it may be that Pd binding leads to a donor atom array "pre-organised" for Ca^{II}, though aside from limited investigations of solution behaviour using ^1H NMR spectroscopy, which indicate that Ca^{II} is much more strongly bound to the pure palladium complex than is K^I, there are presently no data on the issue of any selectivity in this system. The thiophilicity of Pd^{II} is reflected in the relatively small difference between Pd–S [< > 2.261(4) Å] and Pd–O (basal) bond lengths, significantly less here than in the simple palladium complex (< >2.29 cf. 2.00 Å)[10] though the difference is greater than that known in the Pd complex of tetrasulfinylcalix[4]arene, where palladium is bound to the sulfur of one sulfinyl (sulfoxide) entity.[20]

Weak apical-*O* interactions to the palladium atoms are associated with a small degree of twisting of one calixarene entity relative to the other, so that the Pd_2Ca complex provides another example of a chiral ditopic receptor. There is, however, no evidence in the structure of occupancy of the calixarene cavities, neither by CH_2Cl_2 nor by *tert*-butyl CH_3 groups. In this regard, the complex resembles that of Hg^{II}[8] (see below) where again there is a strong distortion of the *cone* towards twofold symmetry (Table S1), such that two opposed phenyl rings are almost parallel, and solvent inclusion is not observed in the solid state (though dmso solvent is present in the lattice and does appear to be involved in $CH_3\cdots\pi$ interactions with the exterior of the calixarene). Any "external" contacts between the Pd_2Ca species, of both the same and the enantiomeric configuration, not mediated by CH_2Cl_2 appear to involve $CH_3\cdots CH_3$ and $CH_3\cdots\pi$ approaches only.

$CaPd(LH_2)_2\cdot H_2O\cdot 3dmso\cdot 4.5MeCN \equiv [\{(dmso\text{-}O)_2(H_2O)\text{-}Ca\}\{Pd(H_2L\cdot 0.5MeCN)(H_2L\cdot MeCN)\}](\cdot dmso\cdot 3MeCN)$ (7b)

While a rational synthesis of **7a** (see Exp. Sect.) on the basis of the stoichiometry established by its structure determination was successful, increasing the ratio Ca/Pd to ca. 1 led to a solution from which two distinctly different crystalline materials deposited. They are also heteronuclear, within a scaffolding of two ligands, but having Pd/Ca 1:1 and Pd/Ca 1:2 ratios, and were obtained from dmso/MeCN solutions, rather than CH_2Cl_2. In both, the Pd coordination environments closely resemble these of **7a**, being planar four-coordinate and comprised of pairs of adjacent phenoxy-*O*,S chelates, with the *O,O′* and *S,S′* pairs *cis* as before. In each case a full formula unit devoid of crystallographic symmetry makes up the asymmetric unit of the structure.

In the 1:1 complex, **7b**, [Figure 10, Table S11, (b)], bond lengths to Pd are very similar to those found in the 2:1 complex [Table S11, (a)]. Within each ligand, O(l11,l31) are assigned as deprotonated; H(l21,l41) are directed toward O(131) with appropriately short O···O distances (Table S1). The calcium coordination sphere is rather heterogeneous and unsymmetrical, with two dmso and one water molecules providing *O*-donors in addition to two *O*-donors from one calixarene and one from the other. The Ca–O bonds [2.404(2), 2.369(2) Å] involving *O*-bridging to Pd are shorter than the bond to the unidentate phenolic-*O* (2.489(3) Å, though the binding to this oxygen atom ap-

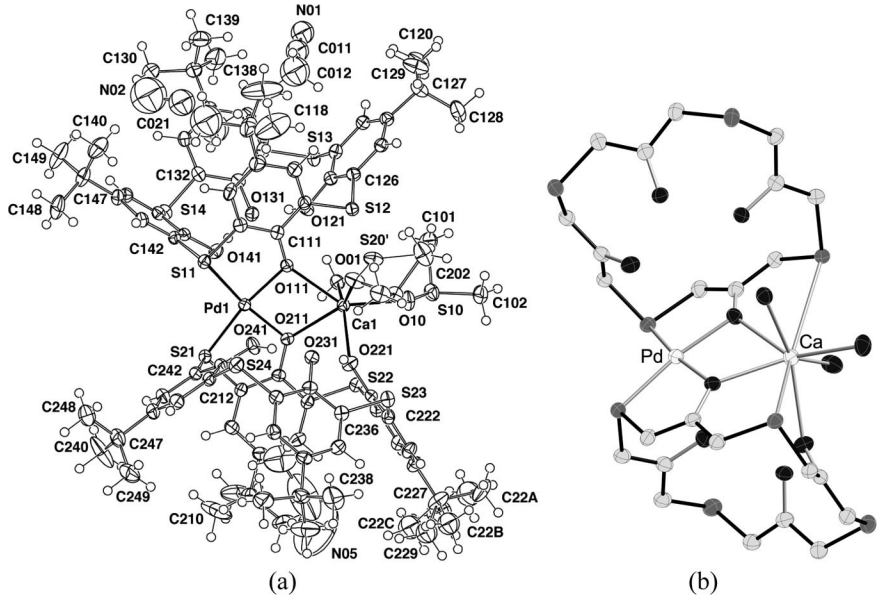

Figure 10. (a) Projection of the heterobinuclear array of $[\{(dmso\text{-}O)_2(H_2O)Ca\}\{Pd(H_2L\cdot 0.5MeCN)(H_2L\cdot MeCN)\}](\cdot dmso\cdot 3MeCN)$ (**7b**). Pd–S;O are 2.2571(8), 2.2727(8); 2.009(2), 1.999(2) Å; Ca–O(111,211,221) are 2.404(2), 2.369(2), 2.489(3); Ca–O(H_2) 3.369(3), Ca–O(dmso) 2.292(3), 2.313(2). Ca···Pd is 3.4323(9) Å. (b) A simplified, perspective view of the coordination core.

pears to enhance interaction with its adjacent sulfur [Ca–S 3.147(1) Å], bringing it somewhat closer than the bound sulfur of the other calixarene [at 3.366(1) Å]. With the asymmetry at the calcium atom, the complex is necessarily chiral, though even ignoring this factor, it would have at most 2-symmetry. The calixarene conformations are much closer to a regular *cone* than those in the 2:1 complex but again (Table S1) the phenyl ring to which the donor atoms bound to Pd are attached is the one most steeply inclined to the mean O_4 plane of the whole ligand. Solvent inclusion is now observed, though the change of solvent vitiates any true comparison with the 2:1 complex.

$Ca_2Pd(LH)_2·1.5H_2O·3.5dmso·4MeCN$ ≡ [{(dmso-*O*)$_2$Ca}-{(dmso-*O*)$_{0.5}$(H_2O)$_{0.5}$Ca}{Pd (HL)$_2$}](·H_2O·4MeCN·dmso) (7c)

The 1:2 Pd/Ca complex **7c** is again a multimetal group sandwiched between a pair of calixarene units (Figure 11). The palladium atom is once again square-pyramidal five-coordinate, with a long apical bond [2.870(3) Å] to a phenolic-*O* and other dimensions of the *cis*-PdO_2S_2 unit [Pd–O 1.991(3), 1.996(3); Pd–S 2.295(1), 2.297(1) Å] essentially identical to those found in the other two complexes. Both calcium atoms have irregular O_6S_2 eight-coordination, with

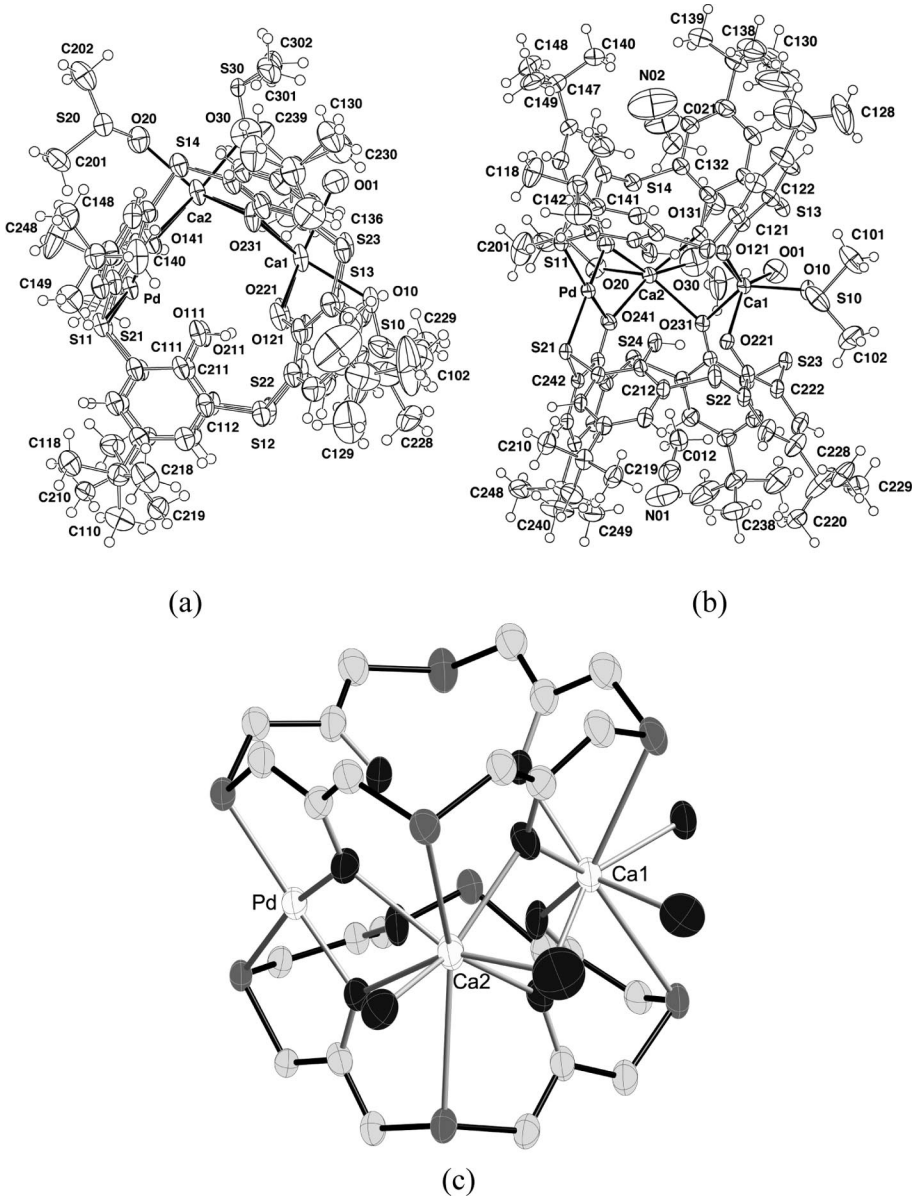

Figure 11. (a), (b) Projections of the heterotrinuclear array of [{(dmso-*O*)$_2$Ca}{(dmso-O)$_{0.5}$(H_2O)$_{0.5}$Ca}{Pd(HL)$_2$}](·H_2O·4MeCN·dmso) (**7c**). Pd–S;O 2.297(1), 2.295(1); 1.996(1), 1.991(3) Å. Ca(1)–O(121,221), Ca(2)–O(131,231) are 2.358(3)–2.393(3); Ca(1)–O(131,231), Ca(2)–O(141,241) are 2.410(3)–2.439(3) Å. Ca–O(H_2) is 2.529(4), Ca–O(dmso) 2.300(6)–2.459(3) Å. Pd···Ca(2) is 3.526(1) Å. (c) Simplified, perspective view of the coordination core.

rather heterogeneous and different arrays of *O*-donors (including water and dmso) on each, and with significantly shorter distances to sulfur on Ca(1) [Ca–S 2.890(1), 2.940(1) Å] than on Ca(2) [3.087(1), 3.115(1) Å], the latter Ca being that closer (and bridged to) the Pd; these distances are also appreciably shorter than those in **7a** and **7b**. The whole unit is unsymmetrical but the calixarene cavities are only slightly distorted from a regular *cone* conformation, this being associated with inclusion of acetonitrile. O(111,211) are protonated and do not interact with any metal atoms, H(111,211) hydrogen-bonding to O(121,221). O(121,221) and O(221,231) forming pairs of chelates above and below the plane to Ca(1); O(131,231) also bridge to Ca(2) to chelate it with O(141) and O(241).

Viewed down *a*, sheets parallel to the *bc* plane appear as columns of homochiral complex units, adjacent columns being of opposite chirality. Within a column, calixarene cavities occupied by acetonitrile are in offset confrontation, seemingly involving both N···CH_3 and CH_3···CH_3 contacts across the interface, although the total pattern of interactions involving these entities is more complicated and extends throughout the lattice. Included acetonitrile, for example, is involved in contacts to non-included acetonitrile which forms pairs with antiparallel dipole arrangements. As in simpler systems,[46] there appears to be no justification for regarding inclusion as simply the consequence of guest-cavity interactions.

Conclusions

As for our description of main group metal ion complexes of *p-tert*-butyltetrathiacalix[4]arene,[16] we reserve a more complete analysis of the present work to the time when a broader context is available including structural studies of complexes of the lanthanide metal ions.[17] It should be noted, however, that for the transition metals (and lanthanides) there is a considerable body of work concerning complexes of thiacalixarene derivatives,[2] and that this and past and present work with *p-tert*-butyltetrathiacalix[4]arene justify the conclusion that both thiacalixarene and calixarene ligands should be considered as "cluster keepers"[1] for metal ions. The Ni_{32} species presently described and its Co_{32} analogue[44] provide spectacular illustration of the capacity of the unfunctionalised ligand to provide larger cluster species than do its derivatives. Other notable particular features of the complexes presently studied are the marked conformational distortions seen in the W^{VI} and mixed Pd^{II}/Ca^{II} complexes and the fact that this seems to preclude solvent inclusion, which is otherwise the norm in complexes where the thiacalixarene has a close-to-regular *cone* conformation. In no present case, however, is the conformational change as great as that to the 1,2-*alternate* form seen in a Ti^{IV} complex.[3b] As for main group complexes,[16] the thiacalixarene binds to transition metals in variously deprotonated forms and readily forms crystalline materials incorporating hydrolytic oligomers. This last observation indicates that, as for metal aryloxides in general, there is undoubtedly a field of thiacalixarene coordination chemistry as yet undefined concerning completely anhydrous media.

Experimental Section

Synthesis: Synthetic procedures were diverse and are described for each of the complexes individually; see also the Experimental Section of the preceding paper.[16]

$VO(OH)(LH_2)\cdot 2.5dmf\cdot 2H_2O$ (×2) (1): $[VO(dmso)_5](ClO_4)_2$[47] (950 mg) in dmf (3 mL) was added to a solution of ($LH_4\cdot CHCl_3$) (520 mg) and $N(CH_2CH_3)_3$ (0.5 mL) in dmf (5 mL). Within 1 h, the green-grey solution had turned red in colour and had begun to deposit deep black-violet needle-like crystals which, after 48 h, were collected, washed with ethanol and dried in vacuo. Yield: 610 mg. Crystals suitable for a structure determination were obtained by recrystallisation from hot dmf (20 mg/5 mL). Analysis of the dried bulk material corresponded to the loss of one molecule of dmf and one of water from the crystalline material for $VO(OH_2)(LH_2)\cdot 2dmf\cdot 0.5H_2O$ (×2). $C_{95}H_{135}N_5O_{19}S_8V_2$ (1918.4): calcd. C 57.66, H 6.52, N 2.92, S 13.39; found C 57.9, H 6.9, N 3.4, S 13.1. SQUID magnetometry showed the complex to be diamagnetic.

$WCl_2(L)\cdot 3.5C_6H_6$ (2): Using a standard Schlenk line system, dry toluene (55 mL) was added to a mixture of ($LH_4\cdot CHCl_3$) (500 mg) and WCl_6 (480 mg), at least partial dissolution of both solids to give a black-purple solution occurring immediately. After heating at reflux (under N_2) for 4.5 h, the reaction mixture was filtered to remove a small amount of very insoluble black material and the filtrate volume then reduced to 12 mL. Storage at –20 °C for 10 d resulted in the deposition of black crystals, which were collected, washed with a little cold toluene and dried under nitrogen. Yield: 30 mg. Crystals suitable for a structure determination were obtained on concentrating a solution in benzene by slow evaporation of the solvent at room temperature. Microanalysis indicated that most benzene of crystallisation (defined by the structure solution) was lost on drying to give $Cl_2W(L)\cdot 0.25C_6H_6$. $C_{41.5}H_{45.5}Cl_2O_4S_4W$ (991.3): calcd. C 50.28, H 4.62; found C 50.3, H 4.6.

$Mn(LH_2)\cdot 3.5CH_2Cl_2$ (×2) (3): $[Mn(dmso)_6](ClO_4)_2$[47] (2150 mg) in dmf (25 mL) was added to a solution of ($LH_4\cdot CHCl_3$) (500 mg) and $N(CH_2CH_3)_3$ (0.5 mL) in dmf (50 mL). After 2 d, the light yellow crystalline precipitate was collected, washed with dmf and dried in vacuo. Yield: 610 mg. Analyses of this seemingly crystalline material could only be rationalised in terms of a rather complicated stoichiometry for $Mn(LH_2)\cdot 2.5dmf\cdot dmso\cdot 2.5H_2O$ (×2). $C_{99}H_{149}Mn_2N_5O_{20}S_{10}$ (2159.7): calcd. C 55.07, H 6.95, N 3.24, S 14.85; found C 54.2, H 6.2, N 3.1, S 14.3, and efforts at recrystallisation in fact indicated it to be impure. Thus, the crude material was extracted with CH_2Cl_2 (100 mg in 150 mL), the extract filtered to remove some very insoluble white solid and the filtrate concentrated slowly to provide colourless needle-like crystals suitable for a structure determination. These needles rapidly effloresced when freed of any supernatant solvent.

$Fe_3O(HCO_2)(LH)_2\cdot 2H_2O\cdot 6dmf$ (4): $[Fe(dmso)_6](ClO_4)_3$[47] (490 mg) in dmf (2 mL) was added to a solution of ($LH_4\cdot CHCl_3$) (200 mg) and $N(CH_2CH_3)_3$ (0.2 mL) in dmf (2 mL). A deep brown-violet solution formed and a small amount of a brown precipitate formed immediately but, after 3 d, the only insoluble material took the form of dark violet crystals. After selection of a crystal for a structure determination, these were collected, washed with ethanol and dried in air. Yield: 222 mg. $Fe_3O(HCO_2)(LH)_2\cdot 6dmf\cdot 2H_2O$ =

$C_{99}H_{137}Fe_3N_6O_{19}S_8$ (2139.3): calcd. C 55.58, H 6.45, N 3.93, S 11.99; found C 54.9, H 6.2, N 3.2, S 12.8.

$(Et_3NH)Ni_2(LH)(LH_2)\cdot 2dmf\cdot 2(CH_3)_2CO\cdot H_2O$ (5a): (This synthesis was actually the result of efforts to explore factors, anion coordination, in particular, influencing the nature of the complexes formed, following the characterisation of the hydrolytic oligomer complex **5c**.) Solutions of ($LH_4\cdot CHCl_3$) (500 mg) and $N(CH_2CH_3)_3$ (0.5 mL) in dmf (5 mL) and of $NiCl_2\cdot 6H_2O$ (600 mg) and NH_4Cl (100 mg) in dmf (5 mL) were mixed to give a yellow-green solution. Ethanol was layered on top of this solution, resulting in the slow deposition of an amorphous pale green precipitate beneath a dark green supernatant liquid. After 24 h, the supernatant was withdrawn and layered with acetone to provide dark green crystals used for the structure determination. Yield: 128 mg. The solid effloresces in air to give a pale green powder insoluble in all common solvents. $(Et_3NH)Ni_2(LH)(LH_2)\cdot 2dmf\cdot 2(CH_3)_2CO\cdot H_2O$ = $C_{98}H_{135}N_3Ni_2O_{13}S_8$ (1937.0): calcd. C 60.76, H 7.02, N 2.17; found C 60.5, H 6.7, N 2.1.

$Ni_6(L)(LH)(LH_2)\cdot 4MeCN\cdot 6H_2O$ (5b): (The following is a description of the first efforts made to obtain an Ni^{II} complex of the thiacalixarene.) Solutions of ($LH_4\cdot CHCl_3$) (700 mg) and $N(CH_2CH_3)_3$ (1 mL) in dmf (20 mL) and of $[Ni(dmso)_6](ClO_4)_2$[47,48] (1.5 g) in dmf (10 mL) were mixed to give a final clear yellow-green solution. This was heated (possibly unnecessarily) for 1 h on a steam bath, then cooled, diluted with CH_2Cl_2 (200 mL) and extracted with water (3×200 mL). The aqueous extracts were not perceptibly coloured. The CH_2Cl_2 solution was dried with anhydrous Na_2SO_4, then concentrated to a volume ca. 30 mL. Note that if taken to dryness, this extract provided a powdery yellow-green residue which seemed to be insoluble in most solvents unless, in some cases (e.g. toluene, dichloromethane), extended periods of heating and stirring were applied. Once in solution, simple cooling did not cause precipitation, indicating that dissolution was kinetically limited. By addition of an equal volume of ethanol to the CH_2Cl_2 extract, a precipitate was obtained and by collecting this in six fractions as the CH_2Cl_2 slowly evaporated out, a total of 700 mg of material (ca. 200 mg in the first fraction), ranging in colour from an initial bluish-green to a final yellow-green, was collected. Each fraction was separately dissolved (sometimes by prolonged stirring) in the minimum volume of CH_2Cl_2 and the solutions, after filtration, were then concentrated at room temperature. Each thereby provided some crystalline and some amorphous material but by decanting and rejecting the amorphous material with supernatant solvent and then recrystallising once more from CH_2Cl_2, visually homogeneous solids were obtained in quantities of 20–30 mg each. A crystal originating from the first fraction provided an unsatisfactory structure solution but one indicating a binuclear species to be present, while the fifth fraction provided a crystal containing the hexanuclear species **5b**. Anal. calcd. for $Ni_6(LH)_4\cdot 4CH_3CN$ (a dehydrated form of the species found in the crystal) = $C_{168}H_{192}N_4Ni_6O_{16}S_{16}$ (3388.5): calcd. C 59.55, H 5.71, S 15.14; found C 60.0, H 5.7, S 15.4.

$Ni_{32}(OH)_{40}(L)_6\cdot 8dmso\cdot 10dmf \equiv [Ni_{32}(OH)_{24}(OH)_{16}(L)_6](\cdot 8dmso\cdot 10dmf)$ (5c): $[Ni(dmso)_6](ClO_4)_2$ (2.00 g) in dmf (10 mL) was added to a solution of ($LH_4\cdot CHCl_3$) (200 mg) and $N(CH_2CH_3)_3$ (1 mL) in dmf (3 mL). The green solution formed was filtered into an open tube. Ethanol (10 mL) was layered on top of the filtrate and the mixture was allowed stand open to the atmosphere. After 1 week, a fine, pale green precipitate had formed but, after standing for a further 3 weeks this had transformed into large green crystals. After selection of one for a structure determination, these were collected, washed with ethanol and dried in air. Yield: 250 mg. Elemental analysis of the product thus isolated was consistent with some loss of organic solvents and absorption of water relative to the formulation based on the structure solution. Anal. calcd. for $Ni_{32}(OH)_{40}(L)_6\cdot 4dmso\cdot 8dmf\cdot 30H_2O$ = $C_{272}H_{444}N_8Ni_{32}O_{106}S_{28}$ (8298.8): calcd. C 39.37, H 5.39, N 1.35, Ni 22.63, S 10.82; found C 38.6, H 4.5, N 1.3, Ni 22.1, S 10.0.

In an attempt to conduct a synthesis based on the apparent stoichiometry of the Ni_{32} species, solutions of $[Ni(OH_2)_6](ClO_4)_2$ (190 mg) in dmf (1 mL) and ($LH_4\cdot CHCl_3$) (84 mg) and $N(CH_2CH_3)_3$ (0.40 g) in dmf (1 mL) were mixed to give a clear yellow-green solution. More $N(CH_2CH_3)_3$ (0.75 g) was added to provide the amount of base necessary for the $40OH^-/6Ni$, without any change in the colour of the solution being apparent. Ethanol (10 mL) was then added and the mixture stood in a capped vial at room temp. Within 24 h, an amorphous green precipitate had commenced to form, though only in a small quantity and the mixture seemed unchanged after another 3 weeks of standing. However, on removing the cap and allowing the solvent to evaporate out, large green crystals formed over the next 2 weeks.

$2Cuac_2\cdot Cu_2(L)\cdot dmf\cdot 4.5CH_2Cl_2$ (6) (ac = CH_3CO_2): A solution of ($LH_4\cdot CHCl_3$) (210 mg) in boiling dmf (15 mL) was added to a solution of $[Cu_2(O_2CCH_3)_4(OH_2)_2]$ (200 mg) in dmf (30 mL), causing the colour of the latter to change instantly from blue-green to a dark green-brown. Olive green crystals began to deposit from the solution as it stood to cool and, after 24 h, these were collected and washed with dmf. Yield: 350 mg. For recrystallisation the complex was dissolved in CH_2Cl_2 (10 mL) to which dmf (2 mL) was then added and the solution left in an open flask to allow the dichloromethane to evaporate. (Most of the complex had crystallised in fact by the time the total volume was ca. 5 mL.) Anal. calcd. for $2Cuac_2\cdot Cu_2(L)\cdot 2dmf\cdot 1.5CH_2Cl_2$ = $C_{55.5}H_{73}Cl_3Cu_4N_2O_{14}S_4$ (1481.0): calcd. C 45.01, H 4.97, N 1.89, S 8.66; found C 45.0, H 5.0, N 2.3, S 8.6. To obtain crystals suitable for a structure determination, a portion of this material was dissolved in CH_2Cl_2 and the solution concentrated by slow evaporation of the solvent at room temperature, this procedure resulting in some change in solvation.

$CaPd_2(LH)_2\cdot 1.5CH_2Cl_2$ (7a): This complex was first isolated (and characterised through a crystal structure determination) from what had been intended to be the synthesis of the true Pd^{II} complex (for which an independent preparation is known[10]). Radial chromatography was investigated as a means of purifying the reaction product and it is presumed that gypsum binder in the chromatographic silica may have been the source of the Ca. Subsequently, a rational synthesis, as follows, was developed. A mixture of ($LH_4\cdot CHCl_3$) (100 mg), $[Pd(C_6H_5CN)_2Cl_2]$[49] (45 mg), $[Ca(dmso)_6](ClO_4)_2$[50] (42 mg) and $N(CH_2CH_3)_3$ (0.2 mL) was stirred in $CHCl_3$ (5 mL) for 5 min as a homogeneous red solution formed. This was filtered and the filtrate concentrated by slow (over 1 month) evaporation of the solvent from a loosely sealed flask, thus providing deep red crystals. Negligible colour remained in the 1 mL of supernatant solvent and the yield was therefore assumed to be quantitative. $CaPd_2(LH)_2\cdot 5.5CHCl_3\cdot 2dmso$ = $C_{89.5}H_{107.5}CaCl_{16.5}O_8Pd_2S_{10}$ (2469.9): calcd. C 43.52, H 4.39, S 12.98; found C 43.3, H 4.2, S 12.8. The original crystals suitable for the structure determination were obtained by slow concentration of a solution from material dissolved in CH_2Cl_2.

$CaPd(LH_2)_2\cdot H_2O\cdot 3dmso\cdot 4.5MeCN$ (7b) and $Ca_2Pd(LH)_2\cdot 1.5H_2O\cdot 3.5dmso\cdot 4MeCN$ (7c): ($LH_4\cdot CHCl_3$) (80 mg), $[Pd(C_6H_5CN)_2Cl_2]$ (40 mg) and $[Ca(dmso)_6](ClO_4)_2$ (60 mg) were stirred with a mixture of $N(CH_2CH_3)_3$ (0.3 mL) and dmso (5 mL) until a clear orange solution had formed. CH_3CN (ca. 5 mL) was layered on top of this solution, leading, over 2 d, to the deposition of a mixture of

red (major component) and orange (minor) crystals, one of each type being subjected to crystal structure determinations which modelled the orange complex as **7b** and the red complex as **7c**.

Structure Determinations: General procedures are described in the preceding paper.[16] Final refinement cycles for the majority of determinations recorded in this paper were executed using the SHELXL 97 program,[51] on F^2 (all data); $I_o > 2\sigma(I)$; reflection weights: $[\sigma 2(F2) + (aP)2 + bP)] - 1[P = (F_o^2 + 2F_c^2)]$. CCDC-662593 (**1**), -662594 (**2**), -662595 (**3**), -662596 (**4**), -662597 (**5a**), -662598 (**5b**), -689813 (**5c**), -662599 (**6**), -662600 (**7a**), -662601 (**7b**) and -662602 (**7c**) contain the supplementary crystallographic data for this paper. These data can be obtained free of charge from The Cambridge Crystallographic Data Centre via www.ccdc.cam.ac.uk/data_request/cif.

$VO(OH)(LH_2)\cdot 2.5dmf\cdot 2H_2O$ (×2) ≡ [{(dmf·LH_2)OV(μ-*O*H)}$_2$](·3dmf·$4H_2O$) (1)

$C_{95}H_{131}N_5O_{19}S_8V_2$, M = 2005.4. Monoclinic, space group $P2_1/c$ (C_{2h}^5, No. 14), a = 20.432(2), b = 13.323(1), c = 22.526(3) Å, β = 112.825(1)°, V = 5652 Å^3. D_c (Z = 2) = 1.18$_0$ g cm^{-3}. μ_{Mo} = 3.7 cm^{-1}; specimen: 0.40 × 0.30 × 0.06 mm; $T_{min./max.}$ = 0.84. $2\theta_{max.}$ = 55°; N_t = 84775, N = 12983 (R_{int} = 0.032), N_o = 9613; R_1 = 0.085, wR_2 = 0.32 (a = 0.20).

***Variata*:** Dmf molecules 10, 20 were modelled as disordered over two sets of sites, the components of dmf 10 refining to 0.585(3) and complement, those of dmf 20 to 0.5. Dmf molecule 30 was assigned a site occupancy of 0.5, with remaining electron density in the region modelled as water molecule oxygen atoms [O(01,02); occupancies 0.5], *tert*-butyl groups 14*n*, 34*n* were modelled as disordered, occupancies concerted with that of dmf 10, after trial refinement. Minor solvent and *tert*-butyl components were modelled with isotropic displacement parameter forms, geometries being constrained to idealised values. Phenolic hydrogen atom locations [H(31,41)] were assigned from difference maps.

$WCl_2(L)\cdot 3.5C_6H_6$ ≡ *cis*-[Cl_2W(L)](·3.5C_6H_6) (2)

$C_{61}H_{65}Cl_2O_4S_4W$, M = 1245.1. Triclinic, space group $P\bar{1}$ (C_i^1, No. 2), a = 13.2550(8), b = 13.2892(8), c = 18.5550(10) Å, α = 93.434(1), β = 98.355(1), γ = 117.368(1)°, V = 2842 Å^3. D_c (Z = 2) = 1.45$_5$ g cm^{-3}. μ_{Mo} = 23 cm^{-1}; specimen: 0.45 × 0.10 × 0.07 mm; $T_{min./max.}$ = 0.97. $2\theta_{max.}$ = 58°; N_t = 28075, N = 9028 (R_{int} = 0.024), N_o = 7887; R_1 = 0.034, wR_2 = 0.089 (a = 0.059).

***Variata*:** An instrument failure resulted in a somewhat less-than-complete sphere of data being measured, reducing to a unique set with 83% of the possible on the only available crystal. One of the benzene rings was modelled as disordered over two sets of sites (occupancies set at 0.5; isotropic displacement parameters); one of the benzene molecules is disposed about a crystallographic inversion centre.

$Mn(LH_2)\cdot 3.5CH_2Cl_2$ (×2) ≡ [{$Mn(H_2L\cdot CH_2Cl_2)$}$_2$](·5CH_2Cl_2) (3)

$C_{87}H_{106}Cl_{14}Mn_2O_8S_8$, M = 2142.4. Triclinic, space group $P\bar{1}$, a = 13.186(3), b = 13.410(3), c = 15.271(4) Å, α = 78.809(5), β = 73.171(4), γ = 86.871(4)°, V = 2535 Å^3. D_c (Z = 1) = 1.40$_3$ g cm^{-3}. μ_{Mo} = 8.3 cm^{-1}; specimen: 0.14 × 0.06 × 0.05 mm; $T_{min./max.}$ = 0.83. $2\theta_{max.}$ = 58°; N_t = 25466, N = 12620 (R_{int} = 0.062), N_o = 5931; R_1 = 0.055, wR_2 = 0.12 (a = 0.048).

***Variata*:** Phenolic hydrogen atoms H(11,21) were located and refined in $(x,y,z,U_{iso})_H$. Dichloromethane molecule 3 was modelled as disordered over two sets of sites, occupancies refining to 0.62(2) and complement; molecule 4 is disordered about a crystallographic inversion centre.

$Fe_3O(HCO_2)(LH)_2\cdot 2H_2O\cdot 6dmf$ ≡ [OFe{$Fe(OH_2)$({*O*CHO}/{*O*-dmf})}$_2$(HL·dmf)$_2$](·2dmf) (4)

$C_{99}H_{137}Fe_3N_6O_{19}S_8$, M = 2139.3. Triclinic, space group $P\bar{1}$, a = 13.347(2), b = 20.766(3), c = 20.979(3) Å, α = 77.789(2), β = 76.783(2), γ = 73.336(2)°, V = 5356 Å^3. D_c (Z = 2) = 1.32$_6$ g cm^{-3}. μ_{Mo} = 6.2 cm^{-1}; specimen: cuboid, 0.1 mm; $T_{min./max.}$ = 0.74. $2\theta_{max.}$ = 58°; N_t = 63352, N = 26411 (R_{int} = 0.054), N_o = 14220; R_1 = 0.064, wR_2 = 0.19 (a = 0.103).

***Variata*:** On two of the iron atoms, two of the unidentate sites were modelled as occupied 50:50 by *O*-dmf and *O*-formate (the latter presumed to have been produced by hydrolysis of the former). Phenolic hydrogen atoms H(131,231) were located and refined in $(x,y,z,U_{iso})_H$; water molecule hydrogen atoms were also located and refined with restrained geometries. *tert*-Butyl groups 23, 24 were modelled as rotationally disordered over two sets of sites about their pendants, site occupancies for the components of the former refining to 0.768(4) and complement, and, for the latter, set at 0.5 after trial refinement, as were components of lattice dmf molecules 2–4, all such fragments being refined with isotropic displacement parameter forms. dmf molecules 6, 7 were modelled in terms of components of total occupancy 0.5.

$(Et_3NH)Ni_2(LH)(LH_2)\cdot 2dmf\cdot 2(CH_3)_2CO\cdot H_2O$ ≡ [Et_3NH][Ni_2-(LH_2·Me_2CO)(LH·dmf)]·dmf·Me_2CO·H_2O (5a)

$C_{98}H_{135}N_3Ni_2O_{13}S_8$, M = 1937.0. Monoclinic, space group $P2_1/c$, a = 17.677(1), b = 24.987(2), c = 23.713(2) Å, β = 103.670(2)°, V = 10177 Å^3. D_c = 1.26$_4$ g cm^{-3}. μ_{Mo} = 5.9 cm^{-1}; specimen: 0.43 × 0.52 × 0.15 mm; $T_{min./max.}$ = 0.87. $2\theta_{max.}$ = 65°; N_t = 147225, N = 36800 (R_{int} = 0.088), N_o = 20899; R_1 = 0.062, wR_2 = 0.18 (a = 0.055, b = 16.9).

***Variata*:** Site occupancies of the disordered lattice dmf and the included acetone molecule components refined to very similar values and were refined in concert to 0.684(9) and complement. Site occupancies of the disordered components of *tert*-butyl group 12 refined to 0.753(8) and complement. Site occupancies of the two components of the disordered Et_3NH cation were set at 0.5 after trial refinement. Phenolic hydrogen atoms on O(111,131,231) were clearly located and refined in (x,y,z,U_{iso}). Hydrogen atoms were not located in association with the residue modelled as a water molecule oxygen atom.

$Ni_6(L)(LH)_2(LH_2)\cdot 4MeCN\cdot 6H_2O$ ≡ [{$Ni_4(H_2O)$(L·MeCN)-(LH·MeCN)}{Ni_2(LH·MeCN)(LH_2·MeCN)}](·5H_2O) (5b)

$C_{168}H_{204}N_4Ni_6O_{22}S_{16}$, M = 3496.6. Triclinic, space group $P\bar{1}$, a = 19.4275(8), b = 19.4844(8), c = 29.4760(10) Å, α = 84.114(1), β = 78.570(1), γ = 88.834(1)°, V = 10879 Å^3. D_c = 1.06$_7$ g cm^{-3}. μ_{Mo} = 7.1 cm^{-1}; specimen: 0.30 × 0.20 × 0.20 mm; $T_{min./max.}$ = 0.75. $2\theta_{max.}$ = 58°; N_t = 119277, N = 52866 (R_{int} = 0.073), N_o = 19082; R_1 = 0.086, wR_2 = 0.27 (a = 0.141).

***Variata*:** Data were measured at room-temperature (293 K), crystal degradation occurring at "low"-temperature. Disordered *tert*-butyl group components 12, 14, 21, 23, 43, 44 were modelled over pairs of sites, occupancies set at 0.5 after trial refinement. Large residues in difference maps were modelled as water molecule oxygen atoms (associated hydrogen atoms not located); significant residual density was insusceptible of meaningful modelling and was suppressed using "SQUEEZE".[52] Phenolic oxygen atom protonation was assigned by consideration of ligand geometry and difference map evidence.

$Ni_{32}(OH)_{40}(L)_6$·8dmso·10dmf ≡ $[Ni_{32}(OH)_{24}(OH)_{16}(L)_6]$(·8dmso·10dmf) (5c)

$C_{286}H_{422}N_{10}Ni_{32}O_{82}S_{32}$, M = 8217.0. Monoclinic, space group $P2_1/n$, a = 24.961(1), b = 26.838(1), c = 33.095(1) Å, β = 95.150(1)°, V = 22081 Å^3. D_c (Z = 2) = 1.23$_6$ g cm^{-3}. μ_{Mo} = 15.4 cm^{-1}; specimen (capillary): 0.55 × 0.40 × 0.30 mm; $T_{min/max}$ = 0.75. $2\theta_{max}$ = 50°; N_t = 240327, N = 38907 (R_{int} = 0.073), N_o = 15538; R_1 = 0.11, wR_2 = 0.37 (a = 0.20).

***Variata*:** Data were measured at room-temperature (293 K), crystal degradation occurring at "low"-temperature. All *tert*-butyl groups were modelled as rotationally disordered about their pendant bonds with idealised geometries, site occupancies being set at 0.5 after trial refinement. The hydroxy groups are divided into two types: twenty-four lie on the exterior of the centrosymmetric Ni_{32} cluster with well-defined oxygen atoms O(1–12); associated hydrogen atoms were not located and were included at estimates. On the interior of the cluster, electron density was ill-defined and difficult to model: various possibilities such as carbonate, nitrate, ... were considered and rejected as unconvincing, the final model adopted being a web of bridging hydroxy group oxygen atom fragments O(011–038) each of 1/3 occupancy (associated hydrogen atoms not located), this model resulting in a neutral aggregate. The better resolved solvent residues were modelled in terms of dmso and dmf. Large voids remained, with diffuse residues between the clusters, insusceptible of satisfactory modelling; these were suppressed in the refinement by the program "SQUEEZE".[52] Partially occupied atom fragments were refined with isotropic displacement parameters.

2Cuac$_2$·Cu$_2$(L)·dmf·4.5CH_2Cl_2 ≡ [(ac-*O*,*O*′-*μ*)$_4$(dmf-*O*)Cu$_4$(L·H_2CCl_2)](·3.5CH_2Cl_2) (6)

$C_{55.5}H_{72}Cl_9Cu_4NO_{13}S_4$, M = 1662.6. Orthorhombic, space group $Pnma$ (D_{2h}^{16}, No. 62), a = 29.443(1), b = 22.022(1), c = 11.224(3) Å, V = 7278 Å^3. D_c (Z = 4) = 1.51$_7$ g cm^{-3}. μ_{Mo} = 16.5 cm^{-1}; specimen: 0.65 × 0.38 × 0.10 mm; $T_{min./max.}$ = 0.61. $2\theta_{max.}$ = 58°; N_t = 79730, N = 9664 (R_{int} = 0.064), N_o = 7206; R_1 = 0.064, wR_2 = 0.19 (a = 0.093, b = 25.7).

***Variata*:** The dmf molecule is modelled as disordered about its bonded oxygen atom over two sets of sites related by the crystallographic mirror plane which passes through the oxygen atom [O(30)] [and also through Cu(1,3), S(1,3) and (included) Cl(1,2)]. *tert*-Butyl 24 was modelled as rotationally disordered about the pendant carbon atom over two sets of sites, occupancies set at 0.5 after trial refinement. The carbon C(01) of the included CH_2Cl_2 is disordered about a pair of sites related by the mirror plane. Lattice CH_2Cl_2 (3) was modelled with the chlorine atoms disordered over two sets of sites, occupancies refining to 0.830(4) and complement. CH_2Cl_2 (4) was set with site occupancy 0.5 after trial refinement.

$CaPd_2(LH)_2$·1.5CH_2Cl_2 ≡ [Ca{Pd(HL)}$_2$](·1.5CH_2Cl_2) (7a)

$C_{81.5}H_{93}CaCl_3O_8Pd_2S_8$, M = 1816.3. Triclinic, space group $P\bar{1}$, a = 10.2060(8), b = 13.265(1), c = 32.222(2) Å, α = 92.657(1), β = 91.492(1), γ = 106.180(1)°, V = 4182 Å^3. D_c (Z = 2) = 1.44$_3$ g cm^{-3}. μ_{Mo} = 8.4 cm^{-1}; specimen: 0.45 × 0.20 × 0.20 mm; $T_{min./max.}$ = 0.92. $2\theta_{max.}$ = 58°; N_t = 45694, N = 20338 (R_{int} = 0.020), N_o = 18637; R_1 = 0.043, wR_2 = 0.11 (a = 0.031, b = 13.4).

***Variata*:** Phenolic hydrogen atoms were readily located and refined in $(x,y,z,U_{iso})_H$ in associated with O(n31), directed toward O(n41), on both ligands. Solvent components were modelled as non-included dichloromethane, disordered, with constrained geometries, in three fragments, site occupancies 0.5. The substrate molecule was very well defined except for the central atom which was mysterious. On the basis of refinement behaviour, charge balance, and geometrical considerations, it was eventually assigned as calcium, with possible origins as discussed above.

$CaPd(LH_2)_2$·H_2O·3dmso·4.5MeCN ≡ [{(dmso-*O*)$_2$(H_2O)Ca}{Pd(H_2L·0.5MeCN)(H_2L·MeCN)}](·dmso·3MeCN) (7b)

$C_{95}H_{125.5}CaN_{4.5}O_{12}PdS_{11}$, M = 2021.6. Monoclinic, space group $C2/c$ (C_{2h}^6, No. 15), a = 39.593(5), b = 25.595(3), c = 23.189(3) Å, β = 112.818(2)°, V = 21660 Å^3. D_c (Z = 8) = 1.24$_0$ g cm^{-3}. μ_{Mo} = 4.9 cm^{-1}; specimen: 0.42 × 0.20 × 0.08 mm; $T_{min./max.}$ = 0.78. $2\theta_{max.}$ = 58°; N_t = 127857, N = 27621 (R_{int} = 0.052), N_o = 18400; R_1 = 0.053, wR_2 = 0.17 (a = 0.092, b = 13.5).

***Variata*:** Phenolic hydrogen atoms were located [in association with O(121,141,221,241), directed toward O(131,131,231,231) respectively], and refined in $(x,y,z,U_{iso})_H$. *tert*-Butyl group 22 was modelled as rotationally disordered about the pendant bond over two sets of sites, occupancies refining to 0.729(8) and complement [isotropic displacement parameter forms, also for the included acetonitrile components 1, 2 the geometries of which were idealised (occupancies 0.5), N, C being assigned from refinement behaviour and plausible hydrogen atom locations, also true of acetonitrile 6 modelled as disordered to either side of a common atom located on a crystallographic 2-axis.] The sulfur atom of dmso (2) was modelled as disordered over a pair of "inverted" sites in the familiar way, occupancies set at 0.5 after trial refinement.

$Ca_2Pd(LH)_2$·1.5H_2O·3.5dmso·4MeCN ≡ [{(dmso-*O*)$_2$Ca}{(dmso-*O*)$_{0.5}$(H_2O)$_{0.5}$Ca}{Pd($HL)_2$}](·H_2O·4MeCN·dmso) (7c)

$C_{95}H_{126}Ca_2N_4O_{13}PdS_{11.5}$, M = 2087.3. Triclinic, space group $P\bar{1}$, a = 12.2771(9), b = 17.947(1), c = 24.628(3) Å, α = 95.239(1), β = 92.992(1), γ = 102.630(1)°, V = 5259 Å^3. D_c (Z = 2) = 1.31$_8$ g cm^{-3}. μ_{Mo} = 5.6 cm^{-1}; specimen: 0.40 × 0.36 × 0.32 mm; $T_{min./max.}$ = 0.85. $2\theta_{max.}$ = 58°; N_t = 58251, N = 25165 (R_{int} = 0.027), N_o = 19632; R_1 = 0.081, wR 2 = 0.23 (a = 0.082, b = 27.9).

***Variata*:** Hydrogen atoms associated with the residues assigned as water molecule oxygen atoms were not located; phenolic-hydrogen atoms were located [in association with O(111,211), directed toward (121,221)] but not refinable. *tert*-Butyl groups 11, 14, 22 were modelled as rotationally disordered about their pendant bonds, site occupancies of the two components of group 11 refining to 0.682(7) and complement, 0.763(6) for group 14, while those of component 22 were set at 0.5 after trial refinement. The sulfur atom of dmso 2 was disordered over two sites, occupancies refining to 0.638(3) and complement. dmso 3 (coordinated) was modelled at 50% occupancy in concert with "water molecule oxygen" O(3), the latter, hydrogen-bonded to dmso 4, was also assigned occupancy 0.5. Dmso and disordered *tert*-butyl group geometries were idealised in refinement.

Coda: Ref.[5a] and ref.[8] record brief preliminary communications of the interesting complexes $[Cu_4(L{\cdot}H_2CCl_2)_2](\cdot CH_2Cl_2)$ (**A**) and $[Hg_4L_4](\cdot 2dmso\cdot 2mesitylene)$ (**B**); we take the opportunity to provide more comprehensive descriptions based on reprocessing of the previous data in the present context.

Cu_2L·1.5CH_2Cl_2 (×2) ≡ $[Cu_4(L{\cdot}H_2CCl_2)_2](\cdot CH_2Cl_2)$ (A)

$C_{83}H_{94}Cl_6Cu_4O_8S_8$, M = 1943.1. Monoclinic, space group $P2_1/c$, a = 16.877(1), b = 28.872(2), c = 39.128(3) Å, β = 95.770(1), V = 18969 Å^3. D_c (Z = 8 tetramers) = 1.36$_1$ g cm^{-3} μ_{Mo} = 12.8 cm^{-1} specimen: 0.57 × 0.17 × 0.08 mm; $T_{min./max.}$ = 0.37. $2\theta_{max.}$ = 50°; N_t = 160847, N = 33502 (R_{int} = 0.048), N_o = 13828; R = 0.060, R_w = 0.068.

***Variata*:** T was ca. 300 K. *tert*-Butyl groups 12, 15, 17, 25–28 were modelled as rotationally disordered about their pendant bonds over

pairs of sites, occupancies set at 0.5 (idealised geometries, isotropic displacement parameter forms). Dichloromethane components were modelled as disordered; site occupancies were set at 0.5 for component 5, refining to 0.661(6) and complement for component 6, their geometries being constrained at idealised values.

Hg_2L·dmso·mesitylene (×2) ≡ $[Hg_4(L)_2]$(·2dmso·2mesitylene) (B)

$C_{102}H_{124}Hg_4O_{10}S_{10}$, M = 2633.0. Orthorhombic, space group *Pban* (D_{2h}^4, No. 50), a = 17.764(1), b = 21.016(2), c = 14.929(1) Å, V = 5573 Å^3. D_c (Z = 2 tetramers) = 1.56$_9$ g cm^{-3}. μ_{Mo} = 57 cm^{-1}; specimen: 0.24 × 0.12 × 0.12 mm; $T_{min./max.}$ = 0.57. $2\theta_{max.}$ = 65°; N_t = 88663, N = 10141 (R_{int} = 0.11), N_o = 4168; R_1 = 0.055, wR_2 = 0.18 (a = 0.075, b = 10.6).

***Variata*: *tert*-Butyl group 4n was modelled as rotationally disordered about a pair of sites, occupancies set at 0.5 after trial refinement. The solvent component of the structure, although shown to be dmso/mesitylene (2:1) from NMR studies and modelled thus in the initial study, was modelled here as a disordered composite with a lesser dmso content than originally postulated.

Cu_2L·1.5CH_2Cl_2 (×2) ≡ $[Cu_4(L{\cdot}H_2CCl_2)_2]$(·$CH_2Cl_2$) (A)

In this complex, two full tetrameric complex molecules together with six dichloromethane molecules (the latter modelled without disorder, albeit with high displacement parameters), devoid of crystallographic symmetry, comprise the asymmetric unit of the structure; each ligand models satisfyingly as being fully deprotonated, [the metal atoms being assigned as copper(II)] and contains an included solvent molecule (Figure 12). To a first approximation the Cu_4L_2 array approaches 4/*mmm* symmetry, but degraded by electronic effects associated with the copper(II) environments, the substituent dispositions on the aromatic rings, and the included solvent molecules whose ClCCl planes contain the cone axis and within each molecule lie quasi-normal to each other, so that the putative symmetry is quasi-$\bar{4}2m$ The core of the molecule comprises a Cu_4 array, approached from either side by the two ligands, superimposed on each other in projection down their mutual axis, also the quasi 4-axis of the molecule, each oxygen atom bridging a pair of copper atoms, and each sulfur associated with one, as in the other $[M_4(LH_x)_2]$ systems hitherto defined, with the copper atoms six-coordinate. Despite the lack of crystallographic symmetry, the packing of the molecules in the lattice is interesting (Figure S1, Supporting Information), molecules 1 packing with the molecular axis quasi-parallel to a and molecules 2 quasi-parallel to b. The aromatic planes of each ligand divide as opposed pairs in respect of their inclination to their O_4 (or the central Cu_4) planes (Table S1), so that their cones are "pinched", impacting on the relative dispositions of their oxygen atoms vis-à-vis those of the partner ligand [Figure S1(a)], so that, whereas those associated with the more steeply inclined donor planes lie "outside" the Cu_4 plane in projection down the molecular axis, those associated with the "flatter" planes, lie almost over the Cu···Cu vectors in projection, from one ligand then the other around the Cu_4 ring, consistent with quasi-$\bar{4}2m$ symmetry.

Copper(II), being a system commonly in six-coordinate octahedral environments associated with steric deformations consequent upon its d^9 electron configuration, might be examined in the present context with some interest in that respect. The metal atom environments, numerous in this example (Table S12), although similar, are also somewhat disparate. The largest *"trans"* angle observed is 162.3(2)°, well below the octahedral norm; the smallest [140.1(2)°] is more typically associated with trigonal prismatic stereochemistry, an expectation somewhat fulfilled in the present situation by considering that the pair of sulfur atoms associated with each copper atom lie almost above each other in projection down the molecular axes, and that the oxygen atom pairs viewed similarly would conform, were it not for the consequences of the "pinching" of the calyces described above.

Among the bond lengths about the copper atoms in each molecule, one Cu–S distance is short [< > 2.47(5); range 2.413(3)–2.552(3)(3) Å] and one long [< > 2.78(9); 2.680(3)–2.891(3) Å], while in respect of the Cu–O distances, three are short [< > 1.96(2);

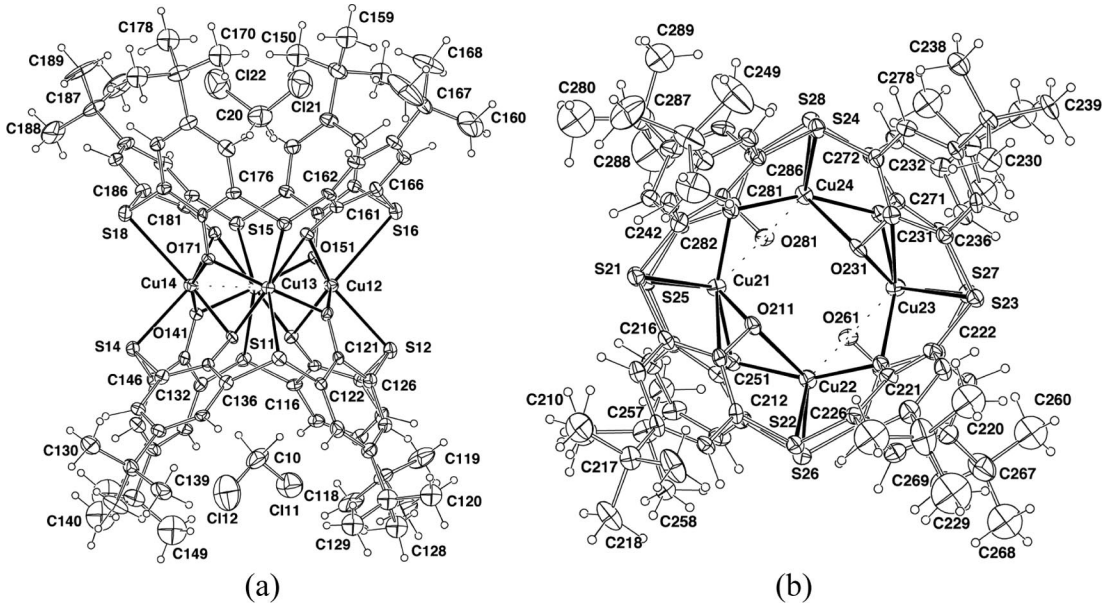

Figure 12. Projections of the two tetramers of $[Cu_4(L{\cdot}H_2CCl_2)_2]$(·$CH_2Cl_2$) (**A**): (a) molecule 1, with included solvent molecules, viewed normal to the (cone) axis; disordered *tert*-butyl components are omitted; (b) molecule 2, without included solvent molecules, projected down the cone axes. Cu–S(short;long) 2.415(3)–2.554(3); 2.680(3)–2.889(3); Cu–O(short;long) 1.929(5)–1.995(5); 2.174(5)–2.431(5) Å; Cu···Cu 2.970(2)–3.053(2) Å.

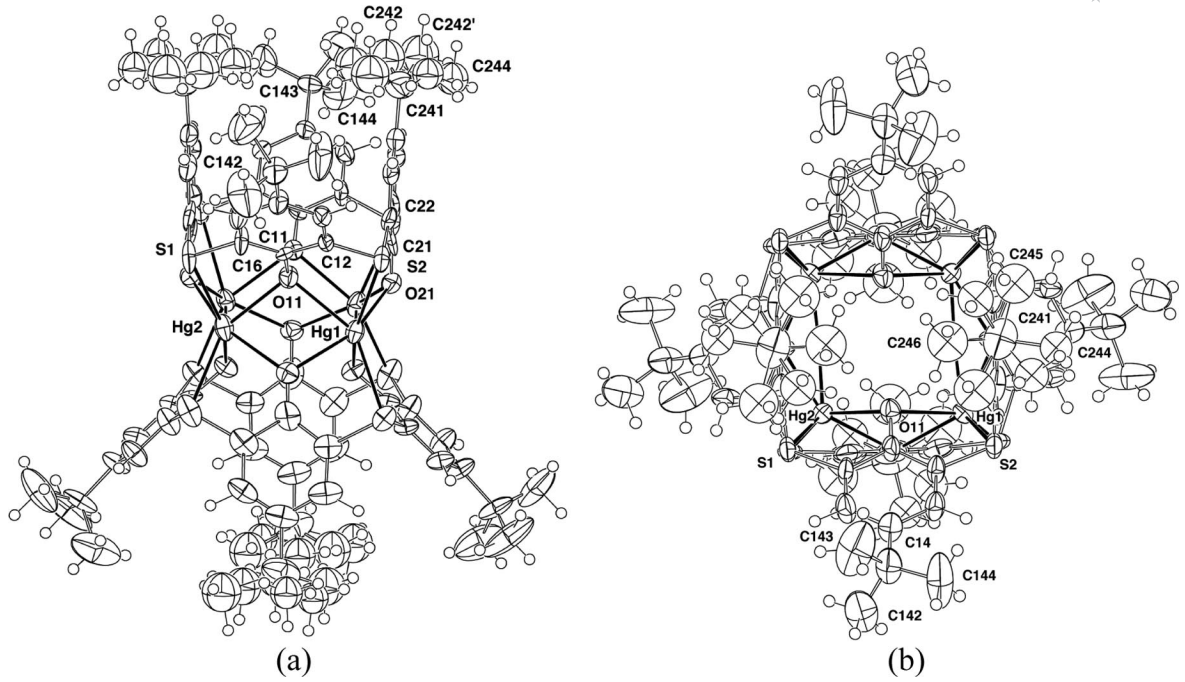

Figure 13. Projections of the tetramer of $[Hg_4L_2]$(·2dmso·2mesitylene) (**B**): (a) normal to and (b) along the cone axis. Hg–S 2.601(1), 2.618(1); Hg–O 2.318(2)–2.455(2). Hg···Hg is 3.7354(3) Å.

1.925(6)–1.994(6) Å] and one long (< > 2.30(10); 2.172(5)–2.431(5) Å. Within molecule 2, a pattern is reasonably clear-cut: the smallest *trans* angles involve both long Cu–O and Cu–S distances and are closely distributed [< > 143.3(9); 142.6(2)–144.2(1)°]; the long Cu–S distances Cu(2n)–S(2n) are to S(21,26,23,28) alternately above and below the Cu_4 plane, while the O–Cu–O angles within the Cu_4O_8 system are the largest or nearly so [all > 155.9(2)°] at O(251,221,271,241). In molecule 1 a different pattern is found: for Cu(11,13), the smallest *trans* angle is again close to 144°, involving long Cu–O,S distances, but for Cu(12,14) the angle is smaller (ca. 140°), involving only one long distance (Cu–S); around the Cu_4O_8 system, large *trans* angles are subtended by O(151,121,171,141).

Hg_4L·dmso·mesitylene (×2) ≡ $[Hg_4(L)_2]$(·2dmso·2mesitylene) (B)

In this complex, a quarter of the formula unit comprises the asymmetric unit of the structure, as modelled in space group *Pban*; the tetranuclear cluster (Figure 13) is well-defined, albeit with one of the *tert*-butyl groups, that associated with aromatic ring 2 of the ligand, being rotationally disordered about the pendant in the frequently observed manner. The accompanying solvent component, modelled as a composite of solvent moieties on the basis of NMR observations, is badly disordered; none of the solvent components are included in the ligand cones. The complex array models satisfyingly in terms of fully deprotonated ligand components in company with Hg^{II}. The cluster overall has crystallographic 222 symmetry about the midpoint of the Hg_4 square at (1/4, 3/4, 0), one 2-axis passing through the pair of Hg(1) which are disposed *transoid* in the Hg_4 square, another through the similarly disposed Hg(2) and the third being the cone axis of the two ligands, the Hg_4 array being exactly square in consequence (Table S13).

Approach to a putative higher symmetry of *mmm* and, beyond this, 4/*mmm*, is broken by the *tert*-butyl disorder, and the dispositions of the aromatic planes of the ligands, which display very different dihedral angles to the O_4/Hg_4 plane(s) (Table S1), so that (Figure 13), the oxygen atoms of the ligand to one side of the Hg_4 plane do not lie in projection over those of the ligand to the other; devoid of the *tert*-butyl groups, the symmetry is quasi-$\bar{4}2m$. Although six-coordinate, the mercury atom environment is far removed from octahedral geometry, the largest *trans*-angles in the coordination sphere lying in the range 144.7(2)–153.0(2)°, more typical of a trigonal-prismatic array, each of these angles involving an O,S pair of donors. Electronically, mercury(II) has a strong affinity for sulfur, as well as a tendency, particularly with "hard" donors, towards two-coordination. The shortest distances about each mercury atom in each case are associated with a pair of quasi-*trans* oxygen donors; nevertheless (see following paper), the metal–sulfur atom distances are relatively rather shorter than those found in other $M_4(LH_x)_2$ systems associated with "harder" metal atoms such as the lanthanides.

Supporting Information (see footnote on the first page of this article): Tables S1–S13, giving descriptors of ligand and metal atom geometry. Figure S1, a view of the lattice of the copper complex **A**.

Acknowledgments

Support from the since extinguished Special Research Centre for Advanced Mineral and Materials Processing and the Crystallography Centre of the University of Western Australia is gratefully recorded.

[1] J. M. Harrowfield, G. A. Koutsantonis in *Calixarenes in the Nanoworld* (Eds.: L. Baklouti, J. M. Harrowfield, J. Vicens), Springer, Dordrecht, **2007**, ch. 10.
[2] T. Kajiwara, N. Iki, M. Yamashita, *Coord. Chem. Rev.* **2007**, *251*, 1734.
[3] Note that we have restricted our considerations to homometallic complexes and cases where only solvent molecules or simple anions are bound to the transition metals in addition to the thiacalixarene. Various complexes containing other strong ligands are known. See, for example, a) D. Brucella, G. D. Par-

kin, *J. Am. Chem. Soc.* **2008**, *130*, 8617; b) J. Zeller, J. Treptow, U. Radius, *Z. Anorg. Allg. Chem.* **2007**, *633*, 741; c) J. Zeller, I. J. Hewitt, U. Radius, *Z. Anorg. Allg. Chem.* **2006**, *632*, 2439. For the unfunctionalised thiacalixarene, a unique example of a mixed metal (Mn/Gd) species is known; d) Y. F. Bi, Y. L. Li, W. P. Liao, H. J. Zhang, D. Q. Li, *Inorg. Chem.* **2008**, *47*, 9733.

[4] N. Iki, N. Morohashi, C. Kabuto, S. Miyano, *Chem. Lett.* **1999**, *28*, 219.

[5] a) G. Mislin, E. Graf, M. W. Hosseini, A. Bilyk, A. K. Hall, J. M. Harrowfield, B. W. Skelton, A. H. White, *Chem. Commun.* **1999**, 373; b) Y. Bi, W. Lao, X. Wang, R. Deng, H. Zhang, *Eur. J. Inorg. Chem.* **2009**, 4989.

[6] A. Bilyk, A. K. Hall, J. M. Harrowfield, M. W. Hosseini, G. Mislin, B. W. Skelton, C. Taylor, A. H. White, *Eur. J. Inorg. Chem.* **2000**, 823.

[7] A. Bilyk, A. K. Hall, J. M. Harrowfield, M. W. Hosseini, B. W. Skelton, A. H. White, *Aust. J. Chem.* **2000**, *53*, 895.

[8] H. Akdas, E. Graf, M. W. Hosseini, A. De Cian, A. Bilyk, J. M. Harrowfield, G. A. Koutsantonis, I. W. Murray, B. W. Skelton, A. H. White, *Chem. Commun.* **2002**, 1042.

[9] N. Morohashi, T. Hattori, T. Yokomakura, C. Kabuko, S. Miyano, *Tetrahedron Lett.* **2002**, *43*, 7769.

[10] H. Katagiri, N. Morohashi, N. Iki, C. Kabuto, S. Miyano, *Dalton Trans.* **2003**, 723.

[11] N. Kon, N. Iki, T. Kajiwara, T. Ito, S. Miyano, *Chem. Lett.* **2004**, *33*, 1046 (A Cu^{II} complex of a dithiacalix[4]arene is reported.).

[12] C. Desroches, G. Pilet, S. A. Borshch, S. Parola, D. Luneau, *Inorg. Chem.* **2005**, *44*, 9112.

[13] C. Desroches, G. Pilet, P. A. Szilagyi, G. Molnàr, S. A. Borshch, A. Boussekou, S. Parola, D. Luneau, *Eur. J. Inorg. Chem.* **2006**, 357.

[14] a) E. Hoppe, C. Limberg, *Chem. Eur. J.* **2007**, *13*, 7006; b) C. Limberg, *Eur. J. Inorg. Chem.* **2007**, 3303.

[15] D.-Q. Yuan, W.-X. Zhu, M.-Q. Xu, Q.-L. Guo, *J. Coord. Chem.* **2004**, *54*, 1243.

[16] A. Bilyk, J. W. Dunlop, A. K. Hall, J. M. Harrowfield, M. W. Hosseini, G. A. Koutsantonis, I. W. Murray, B. W. Skelton, A. H. White, *Eur. J. Inorg. Chem.* **2010**, 2089–2105, preceding paper (Part II).

[17] A. Bilyk, J. W. Dunlop, R. O. Fuller, A. K. Hall, J. M. Harrowfield, M. W. Hosseini, G. A. Koutsantonis, I. W. Murray, B. W. Skelton, A. N. Sobolev, R. L. Stamps, A. H. White, *Eur. J. Inorg. Chem.* **2010**, 2127–2152, following paper (Part IV).

[18] N. Iki, N. Morohashi, T. Suzuki, S. Ogawa, M. Aono, C. Kabuko, H. Kumagai, H. Takeya, S. Miyanari, S. Miyano, *Tetrahedron Lett.* **2000**, *41*, 2587.

[19] T. Kajiwara, S. Yokozawa, T. Ito, N. Iki, N. Morohashi, S. Miyano, *Chem. Lett.* **2001**, *30*, 6.

[20] N. Morohashi, N. Iki, S. Miyano, T. Kajiwara, T. Ito, *Chem. Lett.* **2001**, *30*, 66.

[21] T. Kajiwara, N. Kon, S. Yokozawa, T. Ito, N. Iki, S. Miyano, *J. Am. Chem. Soc.* **2002**, *124*, 11274.

[22] N. Morohashi, N. Iki, M. Aono, S. Miyano, *Chem. Lett.* **2002**, *31*, 494.

[23] N. Kon, N. Iki, S. Miyano, *Tetrahedron Lett.* **2002**, *43*, 2231.

[24] Q. Guo, W. Zhu, S. Dong, S. Ma, X. Yan, *J. Mol. Struct.* **2003**, *650*, 159.

[25] T. Kajiwara, R. Shinagawa, T. Ito, N. Kon, N. Iki, S. Miyano, *Bull. Chem. Soc. Jpn.* **2003**, *76*, 2267.

[26] T. Kajiwara, H. Wu, T. Ito, N. Iki, S. Miyano, *Angew. Chem. Int. Ed.* **2004**, *43*, 1832.

[27] Y. Kondo, K. Endo, N. Iki, S. Miyano, F. Hamada, *J. Inclusion Phenom. Macrocyclic Chem.* **2005**, *52*, 45.

[28] N. Morohashi, F. Narumi, N. Iki, T. Hattori, S. Miyano, *Chem. Rev.* **2006**, *106*, 5291.

[29] Z. Asfari, A. Bilyk, J. W. Dunlop, A. K. Hall, J. M. Harrowfield, M. W. Hosseini, B. W. Skelton, A. H. White, *Angew. Chem. Int. Ed.* **2001**, *40*, 721.

[30] Note that in the case of Ti^{IV}, binding to sulfur does occur when chloride coligands are present but not when the coligand is acetylacetonate – see ref.[3b].

[31] L. Giannini, E. Solari, C. Floriani, N. Re, A. Chiesi-Villa, C. Rizzoli, *Inorg. Chem.* **1999**, *38*, 1438.

[32] W. B. Jennings, B. M. Farrell, J. F. Malone, *Acc. Chem. Res.* **2001**, *34*, 885.

[33] M. W. Hosseini in *Calixarenes 2001* (Eds.: Z. Asfari, V. Böhmer, J. M. Harrowfield, J. Vicens), Kluwer Academic Publishers, Dordrecht, **2001**, ch. 6, p. 110.

[34] J.-C. G. Bünzli, J. M. Harrowfield in *Calixarenes - A Versatile Class of Macrocyclic Compounds* (Eds.: V. Böhmer, J. Vicens), Kluwer Academic Publishers, Dordrecht, **1990**, p. 211.

[35] A. Bilyk, A. K. Hall, J. M. Harrowfield, M. W. Hosseini, B. W. Skelton, A. H. White, *Inorg. Chem.* **2001**, *40*, 672 (Part I: *Systematic Structural Coordination Chemistry of p-tert-Butyltetrathiacalix[4]arene: 1. Group 1 Elements and Congeners*).

[36] M. W. Hosseini in *Calixarenes for Separations, ACS Symposium Series No. 557* (Eds.: G. J. Lumetta, R. D. Rogers, A. S. Gopalan), American Chemical Society, Washington, **2000**, p. 296.

[37] D. A. Buckingham, J. M. Harrowfield, A. M. Sargeson, *J. Am. Chem. Soc.* **1974**, *96*, 1726.

[38] J. M. Harrowfield, B. W. Skelton, A. H. White, F. R. Wilner, *Inorg. Chim. Acta* **2004**, *357/8*, 2358.

[39] N. N. Greenwood, A. Earnshaw, *Chemistry of the Elements*, Pergamon Press, Oxford, **1984**, p. 1266.

[40] G. Aromi, A. R. Bell, M. Helliwell, J. Raftery, S. C. Teat, G. A. Timco, O. Roubeau, R. E. P. Winpenny, *Chem. Eur. J.* **2003**, *9*, 3024.

[41] R. Vilar, *Angew. Chem. Int. Ed.* **2003**, *42*, 1460 and references cited therein.

[42] F. Calderoni, F. Demartin, F. Fabrizi de Biani, C. Femoni, M. C. Iapalucci, G. Longoni, P. Zanello, *Eur. J. Inorg. Chem.* **1999**, 663.

[43] O. A. Gerasko, E. A. Mainicheva, D. Y. Naumov, N. V. Kuratieva, M. N. Sokolov, V. P. Fedin, *Inorg. Chem.* **2005**, *44*, 4133.

[44] Y. Bi, X.-T. Wang, W. Liao, X.-F. Wang, X.-W. Wang, H. Zhang, S. Gao, *J. Am. Chem. Soc.* **2009**, *131*, 11650.

[45] a) T. Tanaka, N. Iki, T. Kajiwara, M. Yamashita, H. Hoshino, *J. Inclusion Phenom. Macrocyclic Chem.* **2009**, *64*, 379; b) N. Iki, M. Ohta, T. Tanka, T. Horiuchi, H. Hoshino, *New J. Chem.* **2009**, *33*, 23; c) N. Iki, M. Ohta, T. Horiuchi, H. Hoshino, *Chem. Asian J.* **2008**, *3*, 849.

[46] Z. Asfari, A. Bilyk, C. Bond, J. M. Harrowfield, G. A. Koutsantonis, N. Lengkeek, M. Mocerino, B. W. Skelton, A. N. Sobolev, S. Strano, J. Vicens, A. H. White, *Org. Biomol. Chem.* **2004**, *2*, 387.

[47] W. L. Reynolds, *Prog. Inorg. Chem.* **1970**, *12*, 1.

[48] E. J. Chan, B. G. Cox, J. M. Harrowfield, M. I. Ogden, B. W. Skelton, A. H. White, *Inorg. Chim. Acta* **2004**, *357/8*, 2365 and references cited therein.

[49] R. A. Walton, *Can. J. Chem.* **1968**, *46*, 2347.

[50] J. M. Harrowfield, W. R. Richmond, B. W. Skelton, A. H. White, *Eur. J. Inorg. Chem.* **2004**, 227.

[51] G. M. Sheldrick, *SHELXL-97: A Program for Crystal Structure Refinement*, University of Göttingen, **1997**.

[52] A. L. Spek, *PLATON*, based on *BYPASS* in P. van der Sluis, A. L. Spek, *Acta Crystallogr., Sect. C* **1990**, *46*, 194.

Received: November 4, 2009
Published Online: April 8, 2010

